Clinical Science (2020) **134** 1887–1909
https://doi.org/10.1042/CS20200168

PORTLAND PRESS

Research Article

Sex diversity in proximal tubule and endothelial gene expression in mice with ischemic acute kidney injury

Jose L. Viñas[1], Christopher J. Porter[2], Adrianna Douvris[1], Matthew Spence[1], Alex Gutsol[1], Joseph A. Zimpelmann[1], Karishma Tailor[1], Pearl A. Campbell[3] and Kevin D. Burns[1]

[1]Division of Nephrology, Department of Medicine, Kidney Research Centre, Ottawa Hospital Research Institute, University of Ottawa, Ottawa, Ontario, Canada; [2]Ottawa Bioinformatics Core Facility, The Sprott Centre for Stem Cell Research, Ottawa Hospital Research Institute, Ottawa, Ontario, Canada; [3]Regenerative Medicine Program, The Sprott Centre for Stem Cell Research, Ottawa Hospital Research Institute, Ottawa, Ontario, Canada

Correspondence: Kevin D. Burns (kburns@toh.ca)

Female sex protects against development of acute kidney injury (AKI). While sex hormones may be involved in protection, the role of differential gene expression is unknown. We conducted gene profiling in male and female mice with or without kidney ischemia–reperfusion injury (IRI). Mice underwent bilateral renal pedicle clamping (30 min), and tissues were collected 24 h after reperfusion. RNA-sequencing (RNA-Seq) was performed on proximal tubules (PTs) and kidney endothelial cells. Female mice were resistant to ischemic injury compared with males, determined by plasma creatinine and neutrophil gelatinase-associated lipocalin (NGAL), histologic scores, neutrophil infiltration, and extent of apoptosis. Sham mice had sex-specific gene disparities in PT and endothelium, and male mice showed profound gene dysregulation with ischemia–reperfusion compared with females. After ischemia PTs from females exhibited smaller increases compared with males in injury-associated genes lipocalin-2 (*Lcn2*), hepatitis A virus cellular receptor 1 (*Havcr1*), and keratin 18 (*Krt18*), and no up-regulation of SRY-Box transcription factor 9 (*Sox9*) or keratin 20 (*Krt20*). Endothelial up-regulation of adhesion molecules and cytokines/chemokines occurred in males, but not females. Up-regulated genes in male ischemic PTs were linked to tumor necrosis factor (TNF) and Toll-like receptor (TLR) pathways, while female ischemic PTs showed up-regulated genes in pathways related to transport. The data highlight sex-specific gene expression differences in male and female PTs and endothelium before and after ischemic injury that may underlie disparities in susceptibility to AKI.

Introduction

Acute kidney injury (AKI) affects up to 5% of hospitalized patients, with a high prevalence in critical care units [1], and there are no effective treatments. Recovery from AKI is associated with adverse outcomes, including a three-fold increased risk of chronic kidney disease (CKD), and a two-fold increase in mortality [2]. In humans, AKI is commonly caused by ischemia–reperfusion injury (IRI), which targets cells of the proximal tubule (PT) leading to necrosis and apoptosis [3,4]. IRI also causes significant endothelial dysfunction, which exacerbates hypoxic injury and contributes to transition to CKD [5].

The majority of experimental studies of kidney IRI has been conducted in male animals, and lack of female data has limited translation for human application [6]. Animal studies suggest that in ischemic AKI, female sex confers protection compared with males [7–10]. This sex dimorphism appears to extend to human AKI. In a United Kingdom database study between 1998 and 2013, men had a 2.19-fold greater risk for dialysis requirement with AKI compared with women [11]. Furthermore, a meta-analysis found that the risk of hospital-associated AKI was significantly greater in men than women, supporting a protective effect of female sex [12].

Received: 14 February 2020
Revised: 09 July 2020
Accepted: 10 July 2020

Accepted Manuscript online: 14 July 2020
Version of Record published: 23 July 2020

Clinical Science (2020) **134** 1887–1909
https://doi.org/10.1042/CS20200168

Sex hormones regulate cellular pathways involved in kidney IRI and have been implicated in defining AKI susceptibility [6–9,13,14]. However, the potential role of sex dimorphism in gene expression remains unexplored. In this regard, significant sex differences in transcriptome profiles have been reported in PTs from healthy mice [15,16], although it is not known if sex differences in the transcriptome occur after ischemic injury. Accordingly, the objective of the present study was to compare renal gene expression profiles in male and female mice with kidney ischemic injury. To identify genes of potential pathophysiologic relevance in kidney IRI, we focused our studies on two cell types that are key targets of ischemic injury: PTs and endothelial cells. Our results demonstrate that females are resistant to kidney IRI, and reveal profound sex disparities in genes with or without IRI. The distinct gene profiles predict alterations in biological processes that may underlie sex differences in AKI susceptibility.

Materials and methods

Kidney ischemia–reperfusion

Seven- to ten-week-old male and female friend leukemia virus B (FVB/N) mice (Charles River Laboratories, Senneville, Quebec, Canada) were anesthetized by inhalation of 1–4% isoflurane (Fresenius Kabi, Toronto, Ontario, Canada), and bilateral kidney IRI was performed as described [17–19]. Briefly, mice were placed on a homeothermic blanket (Harvard Apparatus, Holliston, MA, U.S.A.) to maintain body temperature at 37°C throughout the experiment. After anesthesia, the kidneys were exposed and serrefine surgical clamps were placed on the renal artery and vein of each kidney for 30 min, followed by removal of the clamps (reperfusion). Sham mice were subjected to identical surgery without renal vascular clamping. Mice were killed 24 h after reperfusion for blood and tissue collection. For the present study, all mice were housed in Tecniplast IVC cages within the animal care facility, in a humidified environment (50–70%) with positive air pressure at temperature range of 19–21°C, with full access to food (Envigo Teklad 2018, Envigo, Mississauga, ON, Canada) and water. Female mice were not screened for the stage of the estrus cycle. The surgical procedures were performed at the experimental surgical area of the Animal Care and Veterinary Services at the University of Ottawa. The protocol was approved by the Animal Care Ethics Committee at the University of Ottawa and performed according to the recommendations of the Canadian Council for Animal Care.

Biochemistry

Plasma creatinine levels were analyzed by cation-exchange high-performance liquid chromatography, and plasma urea was measured using a urea assay kit (Abcam, Cambridge, U.K.) [17–19].

Neutrophil gelatinase-associated lipocalin determination

Plasma neutrophil gelatinase-associated lipocalin (NGAL) levels were detected with the Mouse Lipocalin-2/NGAL DuoSet ELISA (R&D Systems, Minneapolis, MN, U.S.A.). Plasma samples were diluted 1:200 and processed according to the manufacturer's instructions.

Histology

Kidneys were fixed in 4% formalin, dehydrated, embedded in paraffin, and stained. Kidney histologic injury scores and neutrophil infiltration were performed as described [17,18]. All histological analyses were conducted in a blinded manner by a renal pathologist. Megalin staining was assessed using a monoclonal mouse antibody, 1:200 (Santa Cruz Biotechnology, Dallas, Texas, U.S.A.), with Alexa488 secondary antibodies (Jackson ImmunoResearch Laboratories, West Grove, PA, U.S.A.). Tubular apoptosis was assayed using the TUNEL Apoptosis Detection Kit (Genscript, Piscataway, NJ, U.S.A.), as described [17,18].

Caspase-3 activity

Caspase-3 activity was measured on 5 mg of kidney tissue, using the Caspase-3 Assay Kit (Abcam) [17,18].

Immunoblots

Kidney lysates were run on PAGE and incubated with antibodies directed against Bcl-2-associated X protein (Bax) and B-cell lymphoma 2 (Bcl2) (1:1000, Cell Signaling, Beverly, MA, U.S.A.) for 16 h at 4°C. Blots were analyzed using ImageJ software (NIH, Bethesda, MD, U.S.A.), and corrected for β-actin loading controls.

Isolation of PTs and renal endothelial cells

Kidneys from mice were removed and decapsulated 24 h after reperfusion, and dissection of PTs was performed as described [19]. Isolation of endothelial cells was performed on digested kidney tissue using $CD31^+$ microbeads [19].

RNA-sequencing

RNA was isolated from PTs or renal endothelial cells from three male and three female mice in each experimental group, using the RNeasy Plus Micro Kit (Qiagen Inc., Toronto, Ontario, Canada). RNA quality was assessed using the Fragment Analyzer (Advanced Analytical Technologies, Inc., Ames, LA, U.S.A.). Only RNA with RQN scores of >7 was selected for further analysis. Library construction was performed with the NEB Next Ultra II RNA Library Prep Kit for Illumina using the polyA mRNA workflow (New England Biolabs Ltd., Ipswich, MA, U.S.A.). For each sample, 20 ng of total RNA was used as input for the library preparation. Following library construction, the 24 samples were sequenced separately and simultaneously to minimize potential sequencing bias. Samples were run on NextSeq 500 (Illumina, San Diego, CA, U.S.A.). A total of six 75 cycle high output flow cells were run to achieve at least 35 million reads per sample.

Gene validation

Validation of selected genes was performed using TaqMan® Gene Expression Assays configured and preplated on TaqMan® Array Plates (Thermo Fisher Scientific, Waltham, MA, U.S.A.). After RNA extraction from kidneys and cDNA preparation, real-time polymerase chain reaction (PCR) was performed using TaqMan Universal Master Mix followed by thermal cycling in an Applied Biosystems 7000 sequence detection system (Foster City, CA, U.S.A.). Eukaryotic 18S rRNA endogenous control was used to normalize differences in RNA levels, and the relative amount of mRNA to 18s was expressed using the $2^{-\Delta\Delta C_t}$ method [20].

Bioinformatics

Following initial sequencing runs, one RNA-sequencing (RNA-Seq) library was excluded from the analysis because of low yield. After completion of sequencing to a depth of at least 35 million reads per library, transcripts were quantified against vM19 of the GENCODE mouse genome annotation using salmon v0.13.1 [21]. Data were loaded into R (v3.6.0) using the tximport library [22] and the gene/count matrix was filtered to retain only genes with five or more mapped reads in two or more samples. Differential expression was assessed using DESeq2 (v1.24.0) [23], calculating size factors independently for PT and endothelial cell libraries. Principal component analysis (PCA) was performed using the DESeq2 plotPCA function, and hierarchical clustering was run using Euclidian distance; both using rlog-transformed count data.

Expression differences were computed separately for PT and endothelial cell libraries, comparing IRI vs sham samples for male and female mice, and comparing male and female libraries for IRI and sham conditions. Fold-changes were calculated using the lfcShrink function, applying the apeglm method (v 1.6.0) [24], and *P*-values were recalculated without filtering for outliers using Cook's cutoff in DESeq2. Lists of significantly changed genes were identified using a q-value (i.e. a Benjamini–Hochberg corrected *P*-value) cutoff of 0.05. Volcano plots were made using EnhancedVolcano, R package version 1.4.0. 2019 (https://github.com/kevinblighe/EnhancedVolcano), and heatmaps using the pheatmap (https://cran.r-project.org/package=pheatmap), R packages. The R script used to generate the results is available at https://github.com/retropc66/Mouse_kidney_IRI_RNA-seq.

Gene Ontology (GO) and functional enrichment analyses were conducted using the DAVID bioinformatics resource [25], Reactome and KEGG pathway database (https://reactome.org), and the g:Profiler tool (https://biit.cs.ut.ee/gprofiler/gost) using significantly changed genes with an absolute fold difference of 2 or greater.

Statistical analysis

Results are expressed as mean ± SEM and were analyzed using two-way ANOVA with Bonferroni's post-test, or Student's *t* test as appropriate. Statistical analyses were performed with GraphPad Prism 5.0 (GraphPad Software, Inc., San Diego, CA, U.S.A.). $P<0.05$ was considered significant.

Results

Effect of kidney IRI in male and female mice

In male and female mice, IRI caused significant elevations in plasma creatinine (Cr) and urea after 24 h, although females had less pronounced increases in Cr (Figure 1A,B).

Plasma NGAL levels were significantly increased in male mice 24 h after IRI compared with sham, but were not significantly affected by IRI in female mice (Figure 1C). Histologic injury was evident in male kidneys 24 h after IRI (mean score 2.60 ± 0.12 vs sham: 0.06 ± 0.03, $P<0.001$), while kidney damage in females was mild (mean score: 0.62 ± 0.11) (Figure 1D). Immunostaining for megalin, a marker of PT injury [26], was markedly decreased in male mice after IRI compared with females (Figure 1E), and neutrophil infiltration was more prominent in males (Figure 1F).

Clinical Science (2020) **134** 1887–1909
https://doi.org/10.1042/CS20200168

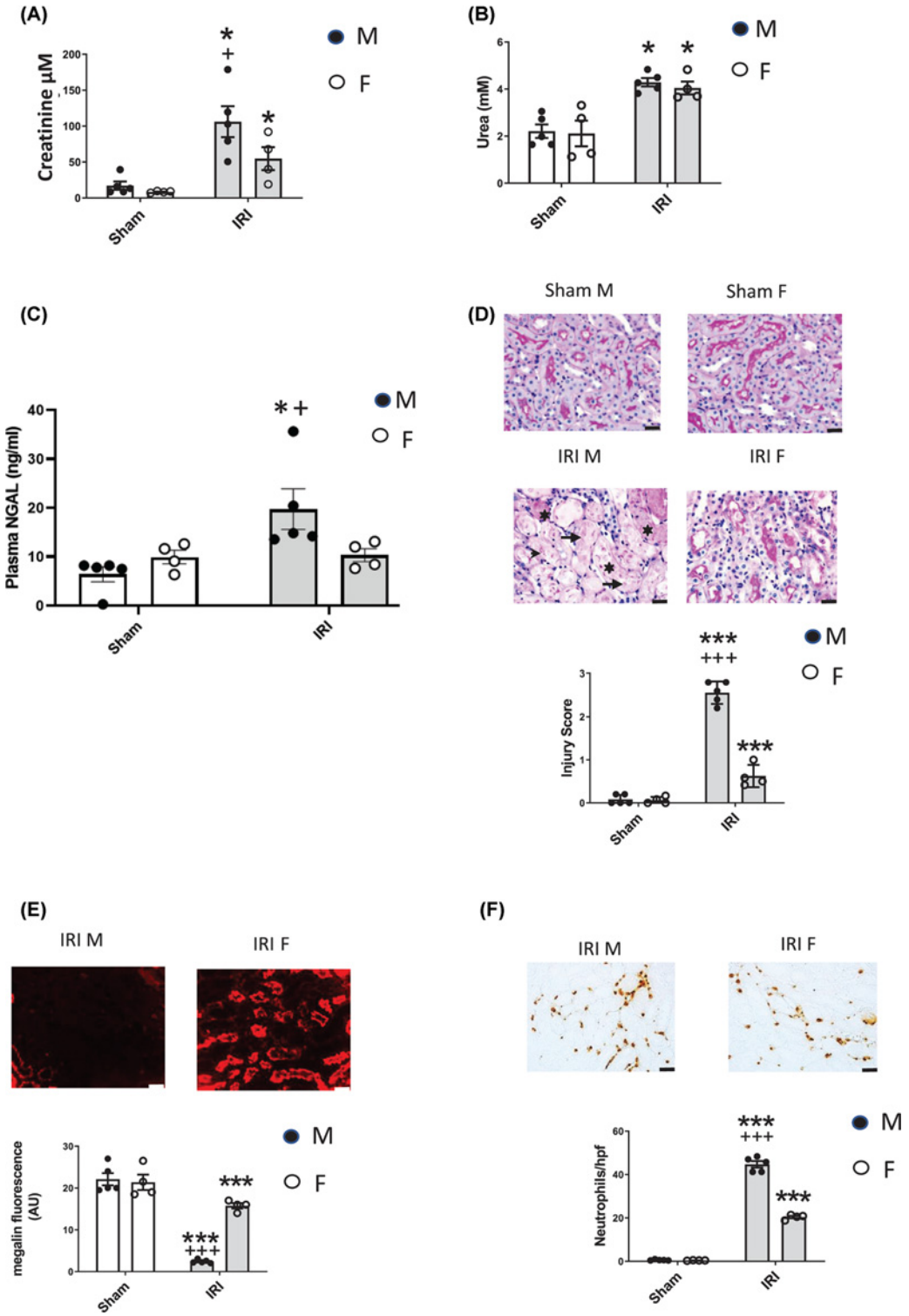

Figure 1. Effect of kidney IRI in male (M) and female (F) mice

Graphs depict effects on (**A**) Plasma Cr, (**B**) Plasma urea, (**C**) Plasma NGAL, (**D**) Kidney histologic injury scores, with representative photomicrographs shown above graph. Arrows: hallmark tubular dilation, asterisks: cast formation, and arrowheads: nuclear loss. Scale, 20 µm. (**E**) Tubular megalin immunostaining, (red fluorescence in arbitrary units (AUs)) with representative images above graph in male and female mice kidneys after IRI. Scale 20 µm. (**F**) Neutrophil infiltration, per high powered field (hpf), with representative images above graph. Scale 20 µm. $^{*}P<0.05$, $^{***}P<0.001$ vs corresponding sham; $^{+}P<0.05$, $^{+++}P<0.001$, all by two-way ANOVA vs corresponding female group; interaction $P<0.05$ for (C) and $P<0.01$ for (D–F); $n=4$ (female) or 5 (male).

Table 1 Top 20 up-regulated and down-regulated genes in sham male compared with sham female mice in proximal tubular cells

Sham M vs F PTs			
Gene symbol	Up-regulated genes log2 fold change	Gene symbol	Down-regulated genes log2 fold change
Gvin1	12.241	Ugt1a2	−9.555
Gstp3	8.731	Cplx3	−9.508
Gm29609	8.539	Atp13a4	−9.368
Styk1	8.422	Slc17a2	−7.327
Adh6b	8.238	Prokr1	−7.208
Gm32687	8.090	Tunar	−6.766
Cyp4f15	7.882	Hdc	−6.502
Zfp365	7.812	E330021D16Rik	−6.459
Smoc1	7.794	Clic6	−6.181
Adamts4	7.748	Prlr	−5.541
Mpped1	7.740	Slc22a29	−5.055
Cldn9	7.378	Cfap77	−4.881
Kdm5d	7.143	Mbl2	−4.784
Gm10409	7.040	Bhmt	−4.780
Nwd2	7.020	Camk1g	−4.743
Gm20537	6.853	Lctl	−4.629
Mlf1	6.823	Gm21973	−4.610
Sorcs1	6.743	Akr1c20	−4.581
Chst12	6.672	Angptl3	−4.566
4930579F01Rik	6.670	Folr2	−4.544

IRI caused greater increases in kidney caspase-3 activity and terminal deoxynucleotidyl transferase-mediated dUTP nick-end labeling (TUNEL) staining in males compared with females (Figure 2A,B). Bax expression increased equally in male and female kidneys after IRI, and Bcl-2 also decreased equally in both sexes (Figure 2C,D).

Transcriptional profiling in sham mice

RNA-Seq was conducted on isolated PTs and renal endothelial cells from male and female mice, either sham-treated or 24 h after IRI, with three biological replicates per experimental group (one sham female endothelial cell library was discarded due to insufficient reads). PCA revealed clustering of RNA-Seq data for both PT (Figure 3A) and endothelial cells (Figure 3B), with clear separation of male and female data.

Comparison between male and female sham mice revealed 1800 differentially expressed genes (DEGs) in PTs (volcano plot Figure 4A, and heatmap Supplementary Figure S1A). Tables 1 and 2 depicts the top 20 up-regulated and down-regulated DEGs in male vs female sham mice, in PTs and endothelial cells. Several DEGs were consistent with recent reports of up-regulated genes in male PT (e.g. acyl-CoA synthetase medium chain family member 3 (*Acsm3*), carboxylesterase 1F (*Ces1f*), cytochrome P450 4B1 (*Cyp4b1*), cytochrome P450 7B1 (*Cyp7b1*), cytochrome P450 2E1 (*Cyp2e1*), and solute carrier family 22, member 30 (*Slc22a30*) and female PT (e.g. solute carrier family 7, member 12 (*Slc7a12*), kynureninase (*Kynu*), prolactin hormone receptor (*Prlr*), and the hormone metabolism genes type I iodothyronine deiodinase (*Dio1*), *GM4450*, osteopontin (*Spp1*), and retinol dehydrogenase 16 (*Rdh16*) [15,16]. Expression of the lipocalin-2 (*Lcn2*) gene, encoding NGAL was significantly increased in sham male PTs compared with females (P=0.006). In sham mouse endothelial cells a smaller number of sex-related DEGs (n=418) was identified compared with PTs (Figure 4B, and heatmap Supplementary Figure S1B). Notably, expression of the vascular markers kinase insert domain receptor (*Kdr*), cadherin-5 (*Cdh5*), *Pecam1* (platelet endothelial cell adhesion molecule (cluster of differentiation 31) [CD31]), and inhibin β B chain (*Inhbb*) [15,27] did not differ between sexes.

Gene profiles with kidney IRI

Heatmaps for DEGs with IRI (compared with sham) in PTs (Figure 5A, 4087 genes) and endothelial cells (Figure 5B, 1025 genes) revealed profound disparities related to sex. As shown on volcano plot, PTs from males showed dysregulation of several genes previously linked to kidney IRI [27–29], including up-regulation of *Lcn2*, hepatitis A virus cellular receptor 1 (*Havcr1*) (*KIM-1*), SRY-Box transcription factor 9 (*Sox9*), keratin 20 (*Krt20*), keratin 18

Clinical Science (2020) **134** 1887–1909
https://doi.org/10.1042/CS20200168

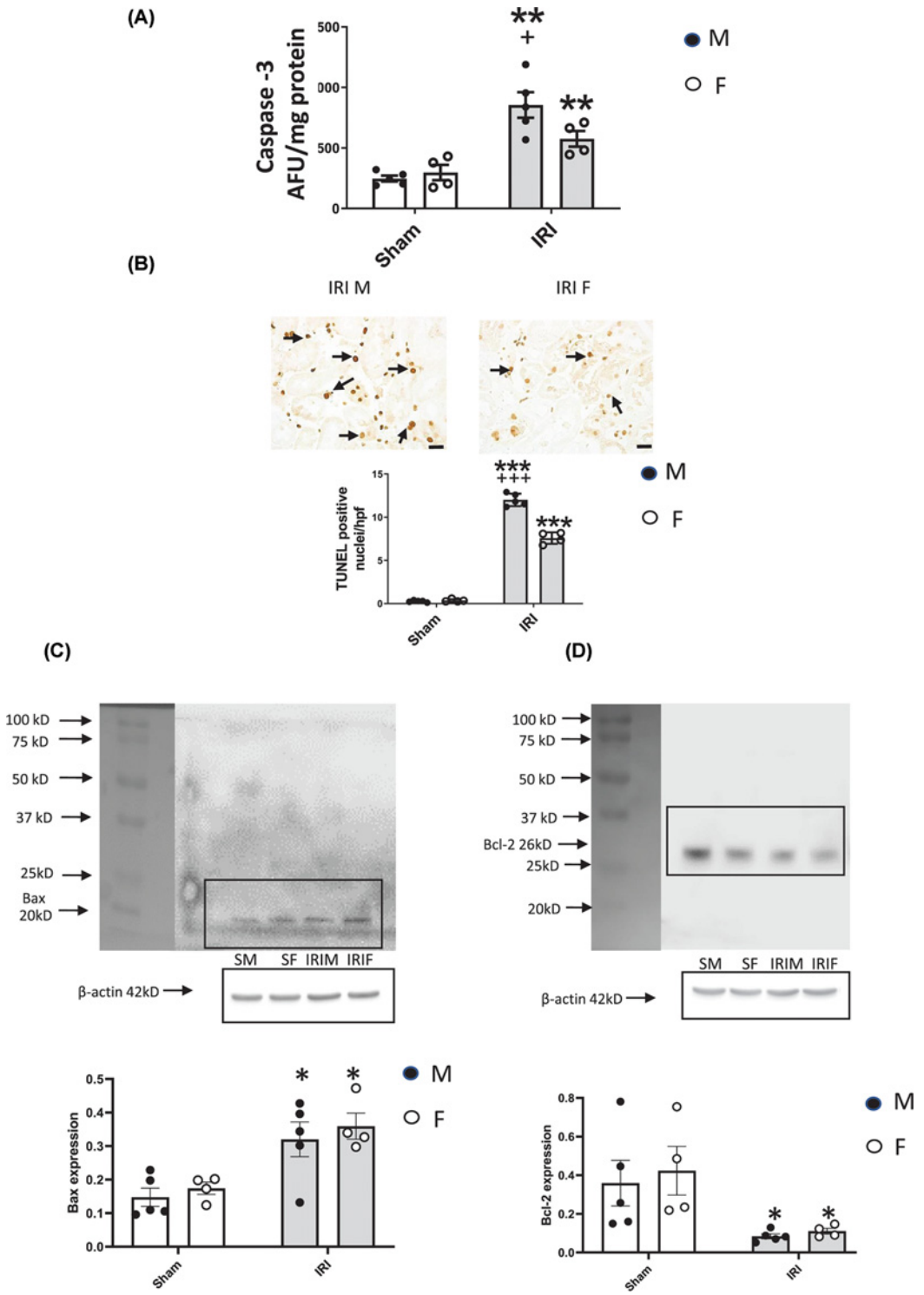

Figure 2. Effect of kidney IRI on apoptosis in male (M) and female (F) mice

(**A**) Kidney caspase-3 activity, (**B**) TUNEL staining, showing positive nuclei per high powered field (hpf); representative photomicrographs are shown above graph after IRI. Arrows: TUNEL-positive nuclei. (**C**) Bax protein expression; representative immunoblot and molecular weight marker from membrane without image development are depicted above graph. (**D**) Bcl-2 protein expression; representative immunoblot and molecular weight marker from membrane without image development are depicted above graph. Black line around each blot indicates that the bands have been grouped together on one membrane. SM; Sham male, SF; Sham female, IRIM; IRI male, IRIF; IRI female. $^{*}P<0.05$, $^{**}P<0.01$, $^{***}P<0.001$ vs corresponding sham, $^{+}P<0.05$, $^{+++}P<0.001$ vs corresponding female group, all by two-way ANOVA; Interaction; $P<0.05$ for A and $P<0.01$ for B; $n=4$ (female) or 5 (male).

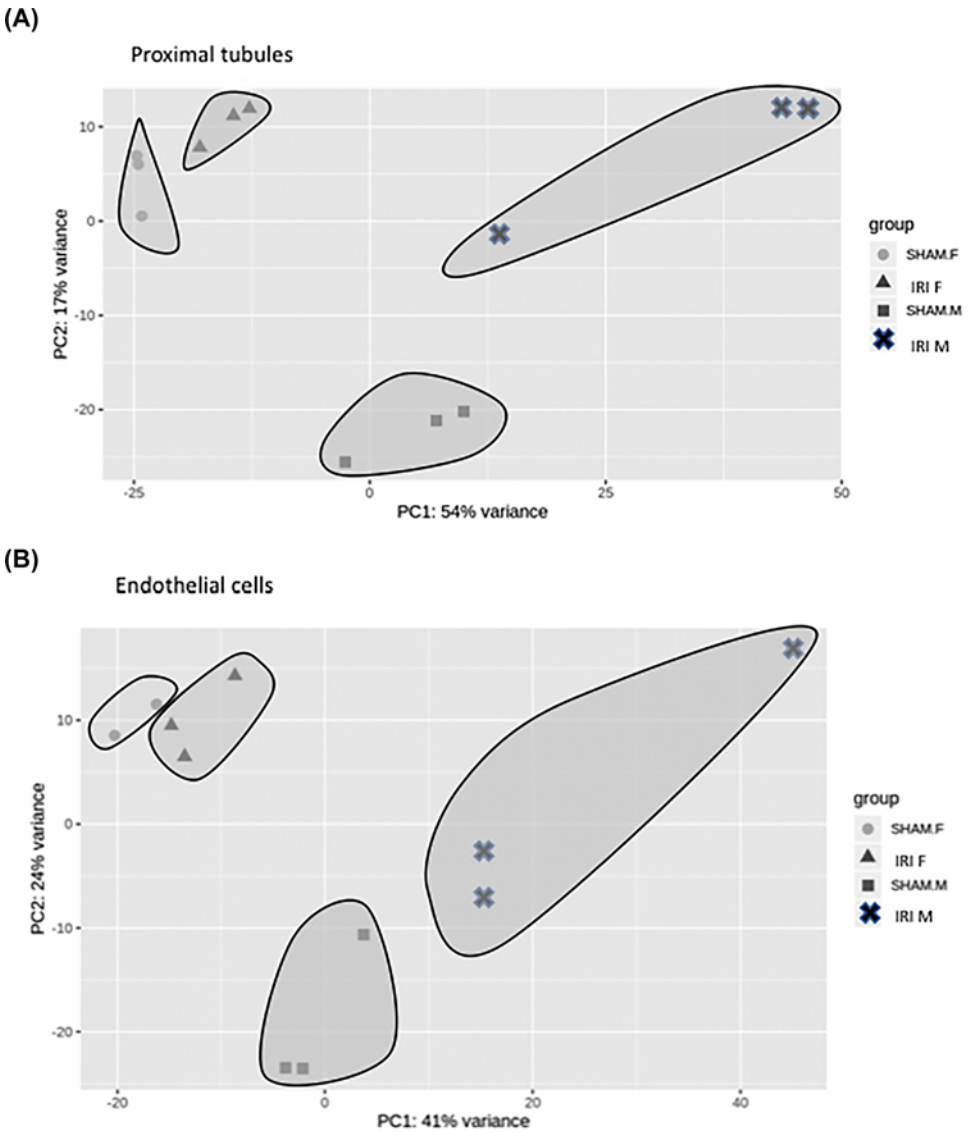

Figure 3. PCA of RNA-Seq data

(**A**) PT RNA-Seq data in male and female mice, with or without kidney IRI. Data segregated into four distinct groups as indicated; n=3 samples per group. (**B**) Renal endothelial cell RNA-Seq data, showing data segregated into four groups; n=3 samples per group, except for female sham group (n=2).

(*Krt18*), *Cldn1* (Claudin 1), and *Clu* (Clusterin), with down-regulation of *Acss2, Slc7a13* and low-density lipoprotein receptor-related protein 2 (*Lrp2*) (megalin) (Figure 6A). Only 488 DEGs were detected in PTs from female mice after IRI compared with sham, and increases in *Lcn2, Havcr1, Clu* and *Krt18* were less prominent than in males (Figure 6B, and heatmap, Supplementary Figure S2). Furthermore, no change occurred in *Sox9*, *Krt20*, or *Cldn,* genes linked to long-term renal injury after AKI [29]. Although *Lrp2* decreased in female PTs post IRI, few other genes were down-regulated.

In endothelial cells, the effect of IRI in both sexes was less pronounced than in PT, with 1025 DEGs in males (Figure 7A) and only 56 DEGs in females (Figure 7B, and heatmap, Supplementary Figure S3). Only male endothelial cells demonstrated up-regulation of adhesion molecules intercellular adhesion molecule 1 (*Icam1*) and *Sele* (E-selectin), and the cytokine C–C motif chemokine 2 (*Ccl2*) and chemokine C–X–C motif chemokine 2 (*Cxcl2*), genes that are associated with enhanced inflammatory infiltration after ischemic injury (P<0.001 for all) [27,29].

A direct comparison of genes between males and females after IRI revealed a large number of DEGs (n=4557) in PTs (Figure 8A), with only 992 DEGs in endothelial cells (Figure 8B, and heatmaps Supplementary Figure S4). Tables

Clinical Science (2020) **134** 1887–1909
https://doi.org/10.1042/CS20200168

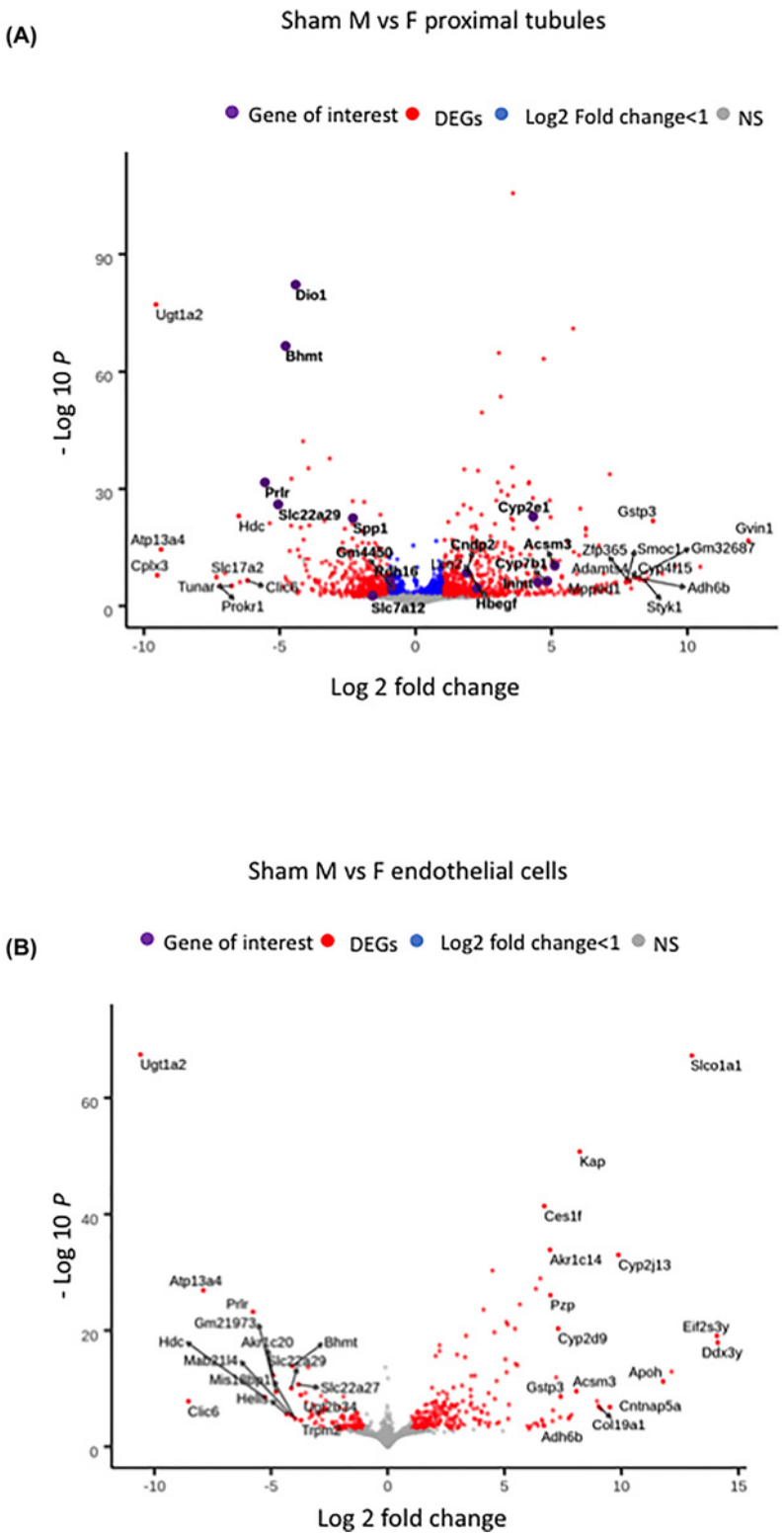

Figure 4. DEGs in sham male and female mice

(**A**) Volcano plot of 1800 DEGs (red) in PTs from sham male mice, compared with sham females. Top up-regulated and down-regulated genes are indicated (arrows), and genes of interest are depicted in purple. (**B**) Volcano plot of 418 DEGs (red) in endothelial cells from sham male mice, compared with sham females. Top up-regulated and down-regulated genes are indicated, and genes of interest are depicted in purple. Blue dots indicate genes in which log2-fold change was <1; gray area includes genes where *P*=NS for differential expression.

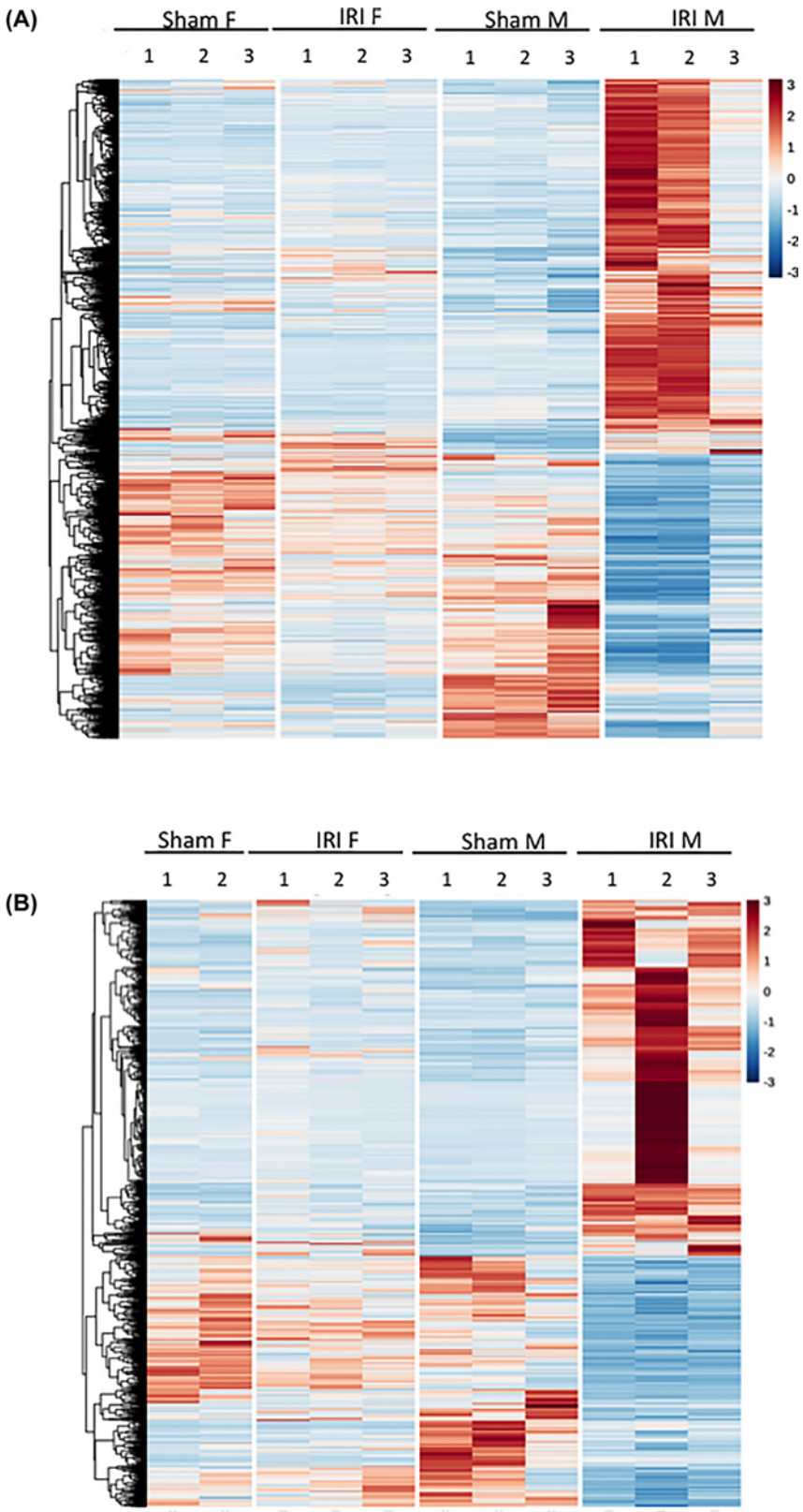

Figure 5. Heatmaps for DEGs from male (M) mice with IRI, compared with sham mice

(**A**) Heatmap for PT DEGs (n=4087) shown for all groups. (**B**) Heatmap for endothelial cell DEGs (n=1025) shown for all groups. Hierarchical clustering of genes indicated at left of each heatmap, and z-score indicated by color; n=3 per group, except for sham female endothelial cells (n=2).

Clinical Science (2020) **134** 1887–1909
https://doi.org/10.1042/CS20200168

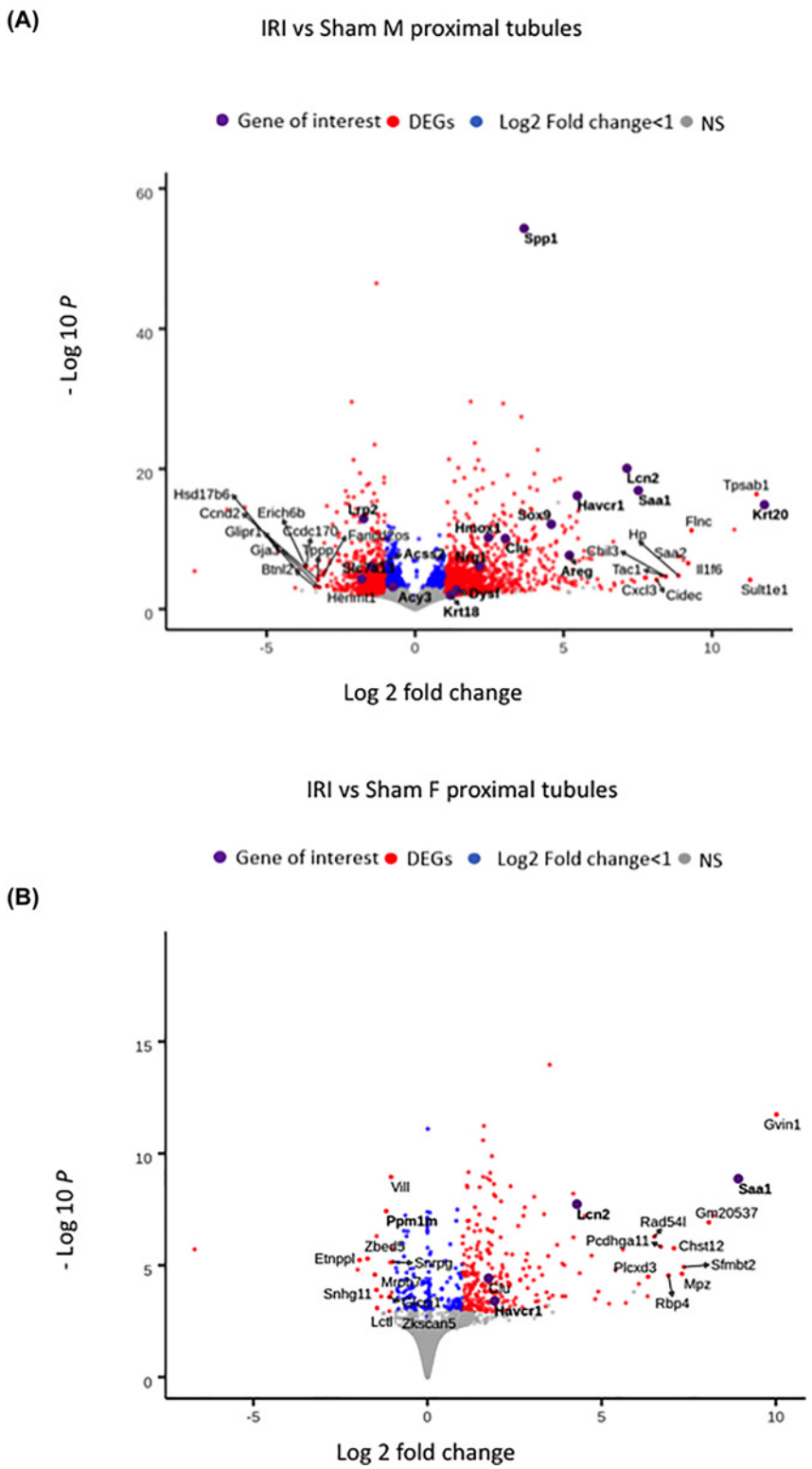

Figure 6. DEGs in mouse PTs with IRI, compared with sham

(**A**) Volcano plot of 4087 DEGs (red) in PTs from male mice with IRI, compared with sham males. Top up-regulated and down-regulated genes are indicated, and genes of interest are depicted in purple. (**B**) Volcano plot of 488 DEGs (red) in PTs from female mice with IRI, compared with sham females. Top up-regulated and down-regulated genes are indicated, and genes of interest are depicted in purple. Blue dots indicate genes in which log2-fold change was <1; gray area includes genes where P=NS for differential expression.

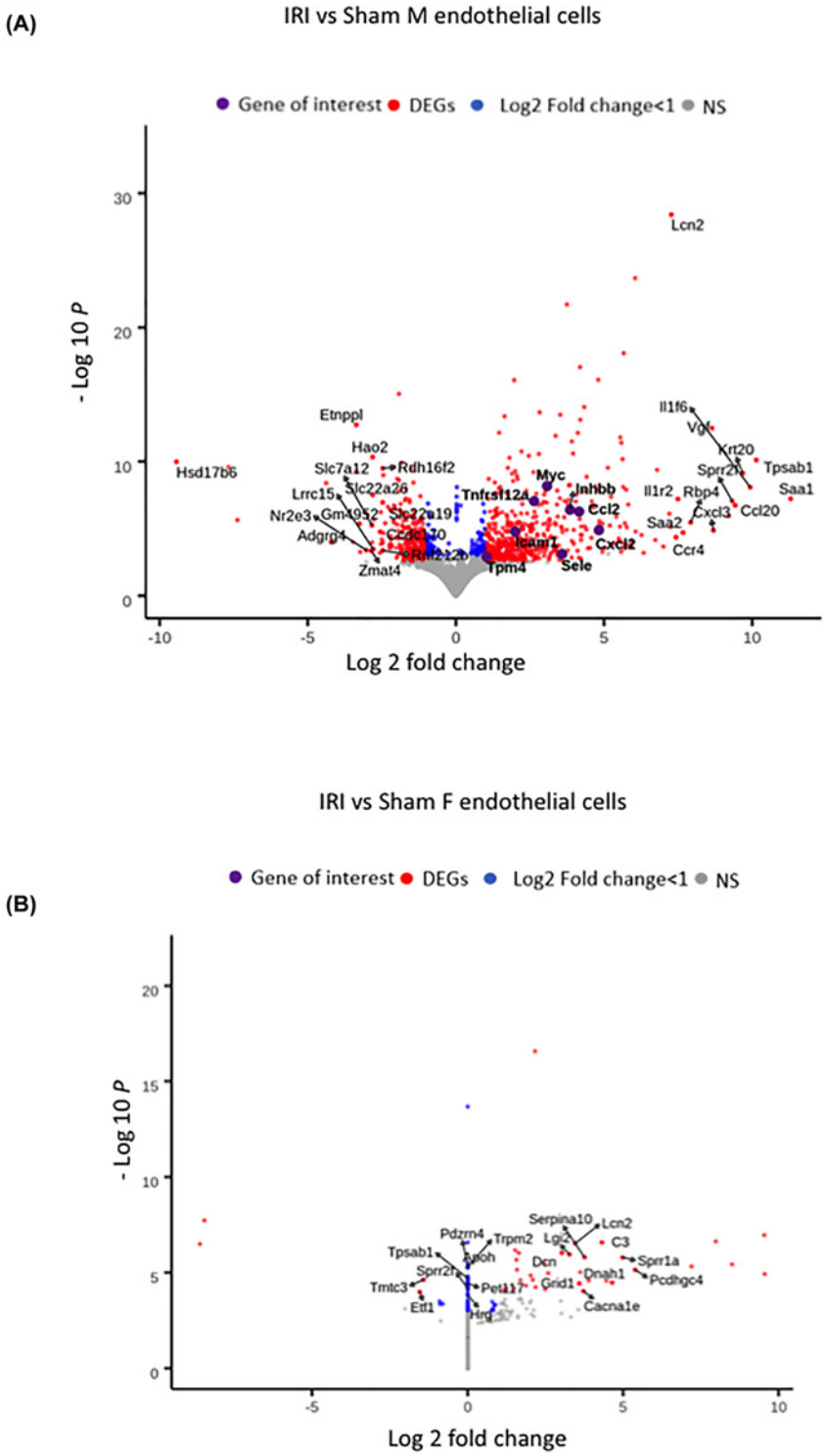

Figure 7. DEGs in mouse renal endothelial cells with IRI, compared with sham

(**A**) Volcano plot of 1025 DEGs (red) in endothelial cells from male mice with IRI, compared with sham males. Top up-regulated and down-regulated genes are indicated, and genes of interest are depicted in purple. (**B**) Volcano plot of 56 DEGs (red) in endothelial cells from female mice with IRI, compared with sham females. Top up-regulated and down-regulated genes are indicated. Blue dots indicate genes in which log2-fold change was <1; gray area includes genes where P=NS for differential expression.

Clinical Science (2020) **134** 1887–1909
https://doi.org/10.1042/CS20200168

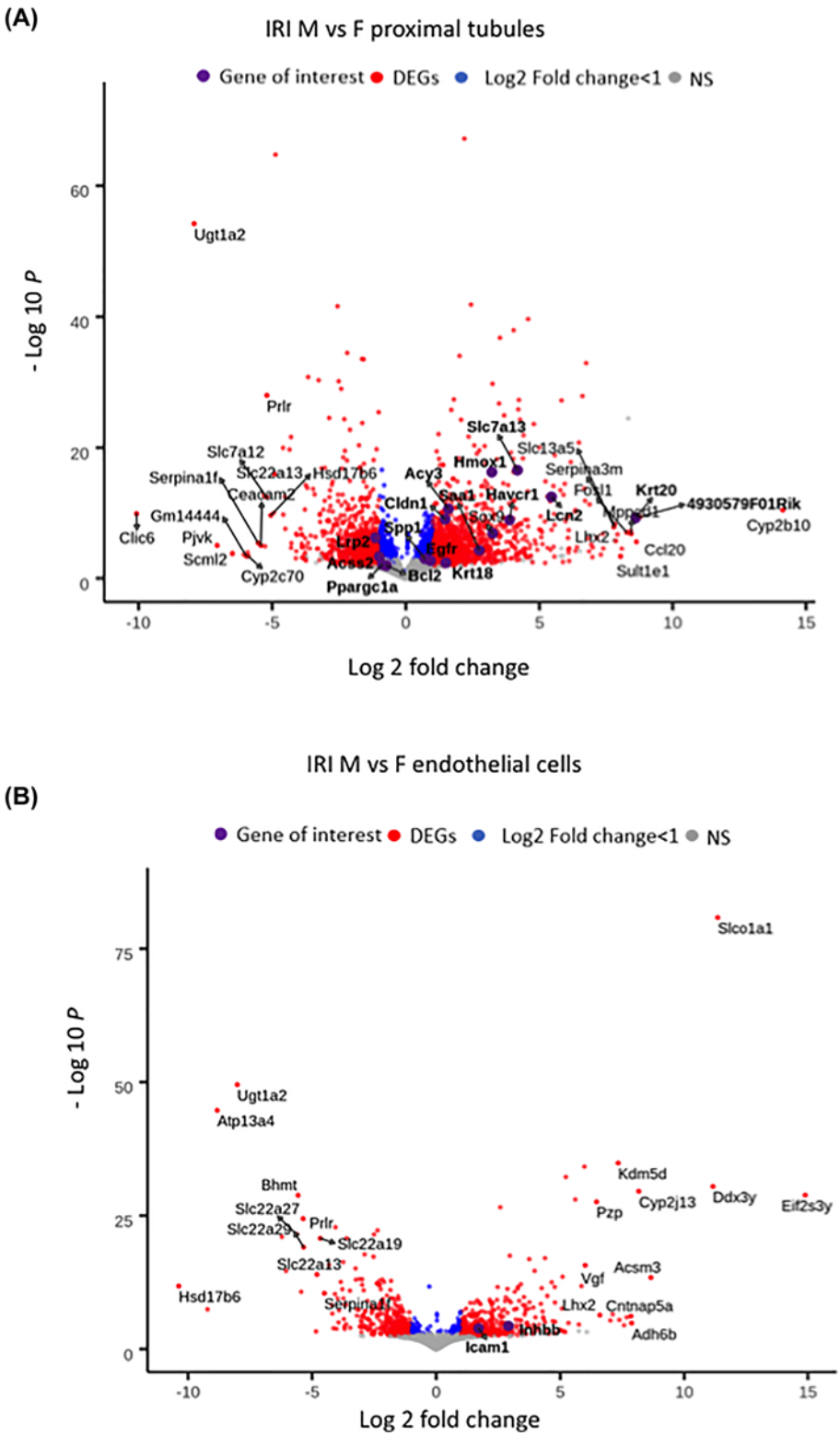

Figure 8. DEGs in males with IRI vs females with IRI

(**A**) Volcano plot of 4557 DEGs (red) in PTs from male mice with IRI, compared with female PTs with IRI. Top up-regulated and down-regulated genes are indicated, and genes of interest are depicted in purple. (**B**) Volcano plot of 992 DEGs (red) in endothelial cells from male mice with IRI, compared with female PTs with IRI. Top up-regulated and down-regulated genes are indicated, and genes of interest are depicted in purple. Blue dots indicate genes in which log2-fold change was <1; gray area includes genes where *P*=NS for differential expression.

Table 2 Top 20 up-regulated and down-regulated genes in sham male compared with sham female mice in endothelial cells

Sham M vs F endothelial cells			
	Up-regulated genes		Down-regulated genes
Gene symbol	log2 fold change	Gene symbol	log2 fold change
Ddx3y	14.112	Ugt1a2	−10.600
Eif2s3y	14.081	Clic6	−8.550
Slco1a1	13.014	Atp13a4	−7.893
Apoh	11.776	Prlr	−5.770
Cyp2j13	9.870	Hdc	−5.281
Cntnap5a	9.503	Akr1c20	−4.913
4930502E18Rik	9.132	Gm21973	−4.788
Col19a1	9.033	Hells	−4.337
Kap	8.218	Slc22a29	−4.135
Acsm3	8.072	Mab21l4	−4.126
Gstp3	7.397	Bhmt	−4.087
Cyp2d9	7.291	Mis18bp1	−3.965
Pzp	6.958	Slc22a27	−3.831
Akr1c14	6.941	Ugt2b34	−3.731
Ces1f	6.701	Trpm2	−3.718
Adh6b	6.685	Cpn1	−3.528
Ugt2b37	6.532	Gsta2	−3.490
Hist1h2bl	6.384	Dio1	−3.413
Kdm5d	6.340	Xpnpep2	−3.357
Ffar3	6.263	Slc22a13	−3.302

Table 3 Top 20 up-regulated and down-regulated genes in IRI male compared with IRI female mice in proximal tubular cells

IRI M vs F PTs			
	Up-regulated genes		Down-regulated genes
Gene symbol	log2 fold change	Gene symbol	log2 fold change
Cyp2b10	14.132	Clic6	−10.071
4930579F01Rik	8.776	Ugt1a2	−7.919
Ccl20	8.633	Pjvk	−7.057
Krt20	8.600	Scml2	−6.487
Mpped1	8.424	Gm14444	−5.967
Fosl1	8.263	Cyp2c70	−5.903
Sult1e1	8.028	Serpina1f	−5.531
Gm10409	7.916	Ceacam2	−5.424
Lhx2	7.839	Slc7a12	−5.215
Serpina3m	7.809	Prlr	−5.195
Slc13a5	7.779	Hsd17b6	−5.046
5830411N06Rik	7.385	Slc22a13	−4.919
Fgf21	7.295	Bhmt	−4.873
Eif2s3y	6.991	Akr1c20	−4.590
Pzp	6.874	Kcnab2	−4.508
Cabp2	6.858	Slc22a29	−4.349
Gstp3	6.744	Slc22a27	−4.294
Lif	6.708	Wdfy4	−4.280
Kdm5d	6.607	Gm1123	−4.111
Ugt2b37	6.476	Kcnj3	−4.099

3 and 4 show the top 20 up-regulated and down-regulated DEGs in males vs females after IRI, in PTs and endothelial cells. Comparing PT DEGs after ischemic injury, males had significant up-regulation of *Havcr1, Lcn2, Sox9, Cldn1*, and *Krt20* compared with females. *Lrp2* was decreased in males compared with females, while epidermal growth factor receptor (*Egfr*) was increased in male PTs, suggesting possible involvement in increased susceptibility to ischemic AKI (P=0.013) [30]. The gene encoding peroxisome proliferator-activated receptor γ co-activator 1-α

Clinical Science (2020) **134** 1887–1909
https://doi.org/10.1042/CS20200168

Table 4 Top 20 up-regulated and down-regulated genes in IRI male compared with IRI female mice in endothelial cells

IRI M vs F endothelial cells			
	Up-regulated genes		Down-regulated genes
Gene symbol	log2 fold change	Gene symbol	log2 fold change
Eif2s3y	14.892	Hsd17b6	−10.372
Slco1a1	11.349	Atp13a4	−8.826
Ddx3y	11.158	Ugt1a2	−8.014
Acsm3	8.656	Slc22a27	−5.627
Cyp2j13	8.168	Bhmt	−5.565
Adh6b	7.881	Gm21973	−5.442
Cntnap5a	7.851	Prlr	−5.363
Gm20671	7.578	Slc22a29	−5.347
4930579F01Rik	7.390	Slc22a13	−4.803
Kdm5d	7.341	Slc22a19	−4.669
Lhx2	6.594	Serpina1f	−4.506
Pzp	6.461	Slc22a26	−4.320
Vgf	6.003	Xpnpep2	−4.203
Kap	5.972	Clic6	−4.186
Ptpn22	5.855	Rdh16f2	−4.058
Hhipl2	5.749	Adgrg4	−4.020
Akr1c14	5.603	Ceacam2	−3.933
Acod1	5.332	Gltpd2	−3.916
Ces1f	5.224	Kynu	−3.845
Nptx2	5.197	Baat	−3.779

(PGC1α) (*Ppargc1a*), implicated in IRI pathogenesis [31,32], was down-regulated in males (P=0.036). With regard to apoptotic genes, *Bcl2* decreased in male PTs after IRI (P=0.047), while *Bax* expression was not significantly different. In endothelium, males had increased expression of AKI-related genes *Icam1* and *Inhbb* [15,27] compared with females after IRI.

Validation of RNA-Seq data

Real-time PCR was performed on kidney tissue for three genes from sham male and female mice, and four genes from males with IRI. These genes were arbitrarily selected, based on previously reported differences between kidneys from healthy males and females or in mice with kidney IRI [15,16,28,29]. The results of PCR were in agreement with RNA-Seq data (Figure 9).

GO

We conducted GO and pathway analysis on DEGs. In sham mice, there was sex disparity for the 20 most significant GO terms associated with up-regulated and down-regulated genes in PTs and endothelial cells (Supplementary Figures S5 and S6). Sham female PTs showed distinct up-regulation of 16 genes involved in cytochrome P450/xenobiotic metabolism, compared with males (heatmap, Supplementary Figure S7). With IRI, the top GO term in male PTs included 52 up-regulated genes for inflammatory responses, while down-regulated genes were linked to metabolic processes, including oxidation-reduction (Figure 10A). In PTs from females with IRI, fewer genes were up-regulated, and the top 20 GO terms included positive regulation of cell proliferation, and several transport processes (Figure 10B). Due to the low number of down-regulated genes in female PTs after IRI, no GO terms were identified. In PTs with IRI, heatmaps showed up-regulation of genes involved in tumor necrosis factor (TNF) and Toll-like receptor (TLR) signaling pathways in males (Figure 11A,B), while females had up-regulation of 52 genes involved in transport pathways (Figure 11C).

The top 20 GO terms of up-regulated genes in endothelial cells from males with IRI (compared with sham) included inflammatory responses and angiogenesis. Down-regulated genes were related to oxidation-reduction, and various metabolic processes (Figure 12A). In endothelial cells from female mice with IRI, only three GO terms were identified from ten up-regulated genes (Figure 12B). No GO terms arose for down-regulated genes in female endothelial cells after IRI, due to the small number of DEGs. Heatmaps from male endothelial cells with IRI showed activation of

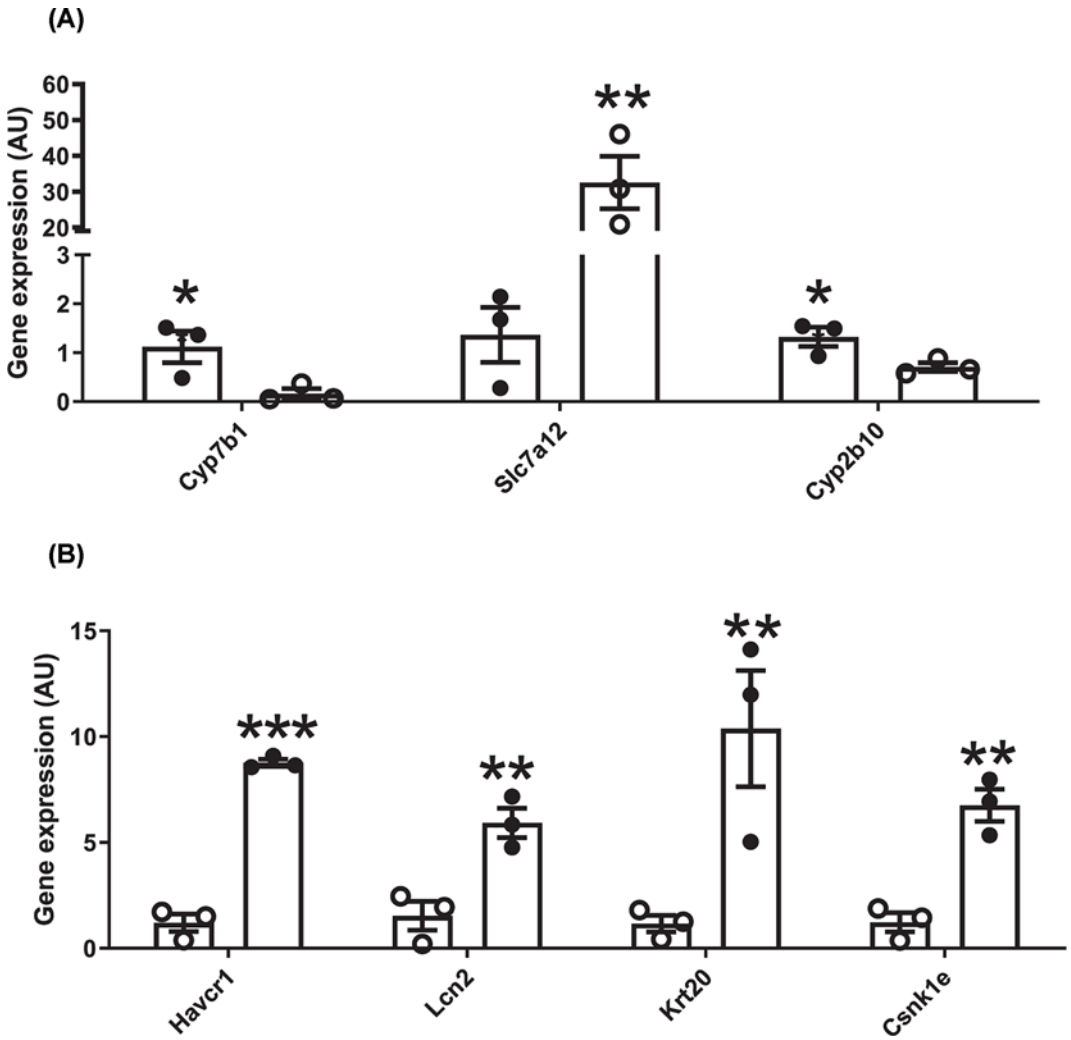

Figure 9. Validation of RNA-Seq

Graphs depict results of real-time PCR (AU, arbitrary units) for (**A**) three genes compared in male (●) and female (○) sham mouse kidneys (*Cyp7b1, Slc7a12, Cyp2b10*), and (**B**) four genes in PTs from male mice, sham (○) vs IRI (●) (*Havcr1, Lcn2, Krt20, Csnk1e*). *$P<0.05$, **$P<0.01$, ***$P<0.001$ vs corresponding group, by Student's *t* test; $n=3$ per group.

genes linked to TNF signaling and cytokine receptor interaction, although there was variability in response between mice (Figure 13).

Discussion

Males are more susceptible to AKI than females, and this sex dimorphism extends to the risk of development of CKD in animal studies and humans. To date, disparities in kidney gene expression between males and females with IRI have not been examined. Here, we found that female mice were protected from kidney IRI compared with males. While it might be expected that increases in plasma Cr should be lower in females after IRI compared with males due to decreased muscle mass, we observed no significant difference in baseline Cr measurements, and other markers of renal damage, including plasma NGAL, histologic injury scores, megalin expression, and neutrophil infiltration demonstrated no change or only a minor degree of injury in female mice. Importantly, using RNA-Seq we report profound sex differences in the transcriptome in mice with and without kidney ischemic injury, within PTs and endothelial cells. Sex-specific gene profiles are predicted to significantly impact molecular pathways involved in AKI pathogenesis and repair, and it is possible that they are involved in the resistance to ischemic AKI in females.

Differences in expression of 1800 PT genes occurred between male and female sham mice, which exceeded numbers of sex-specific DEGs in the endothelium by more than four-fold. Several DEGs in PT were in good agreement

Clinical Science (2020) **134** 1887–1909
https://doi.org/10.1042/CS20200168

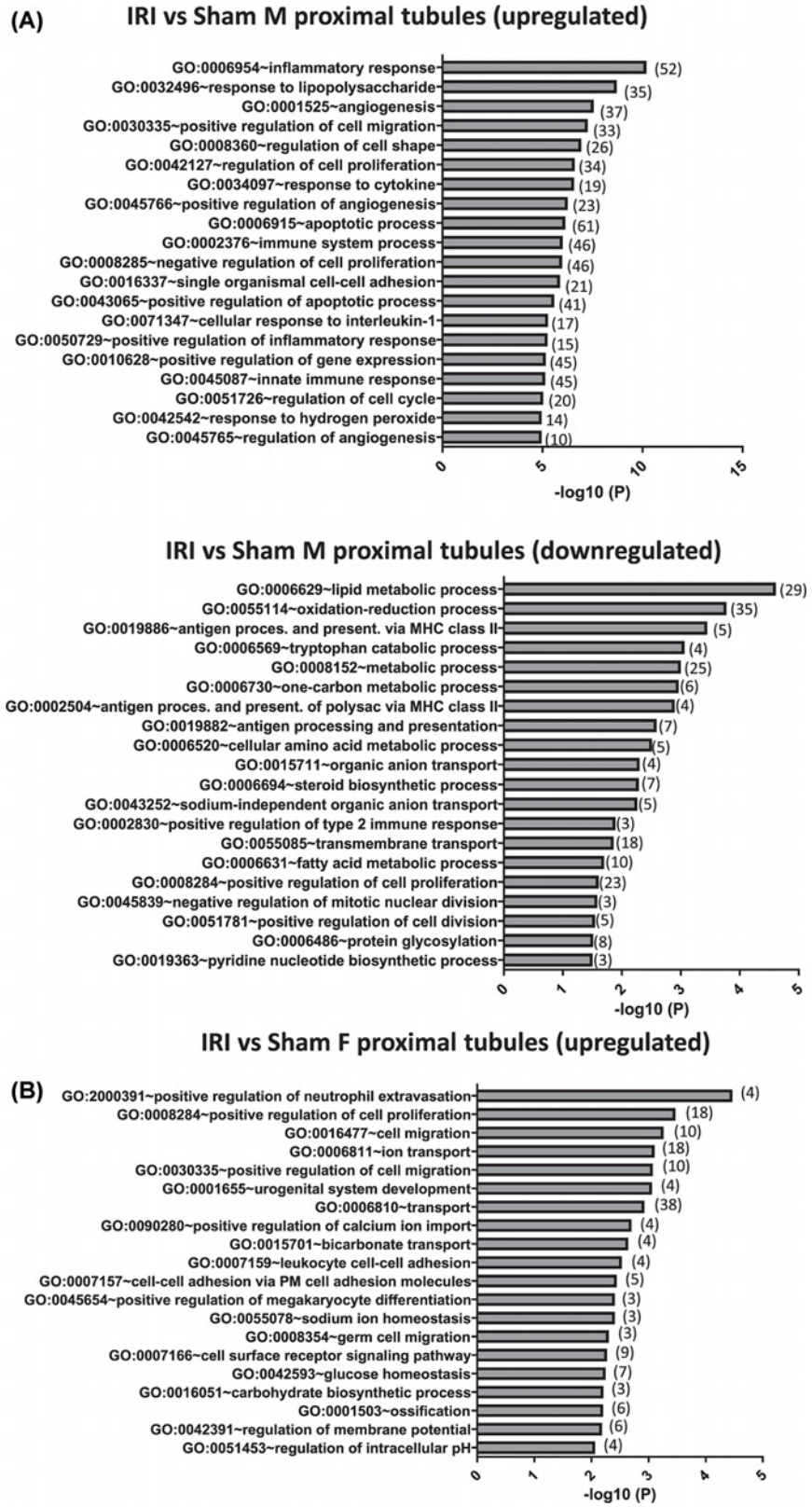

Figure 10. GO terms for up-regulated and down-regulated genes in PTs after IRI

(**A**) Top 20 GO codes and terms for up-regulated and down-regulated genes from males are indicated, ranked according to level of significance, with number of genes in each term in parentheses. (**B**) Top 20 GO codes and terms for up-regulated genes from females are indicated, ranked according to level of significance, with number of genes in each term in parentheses.

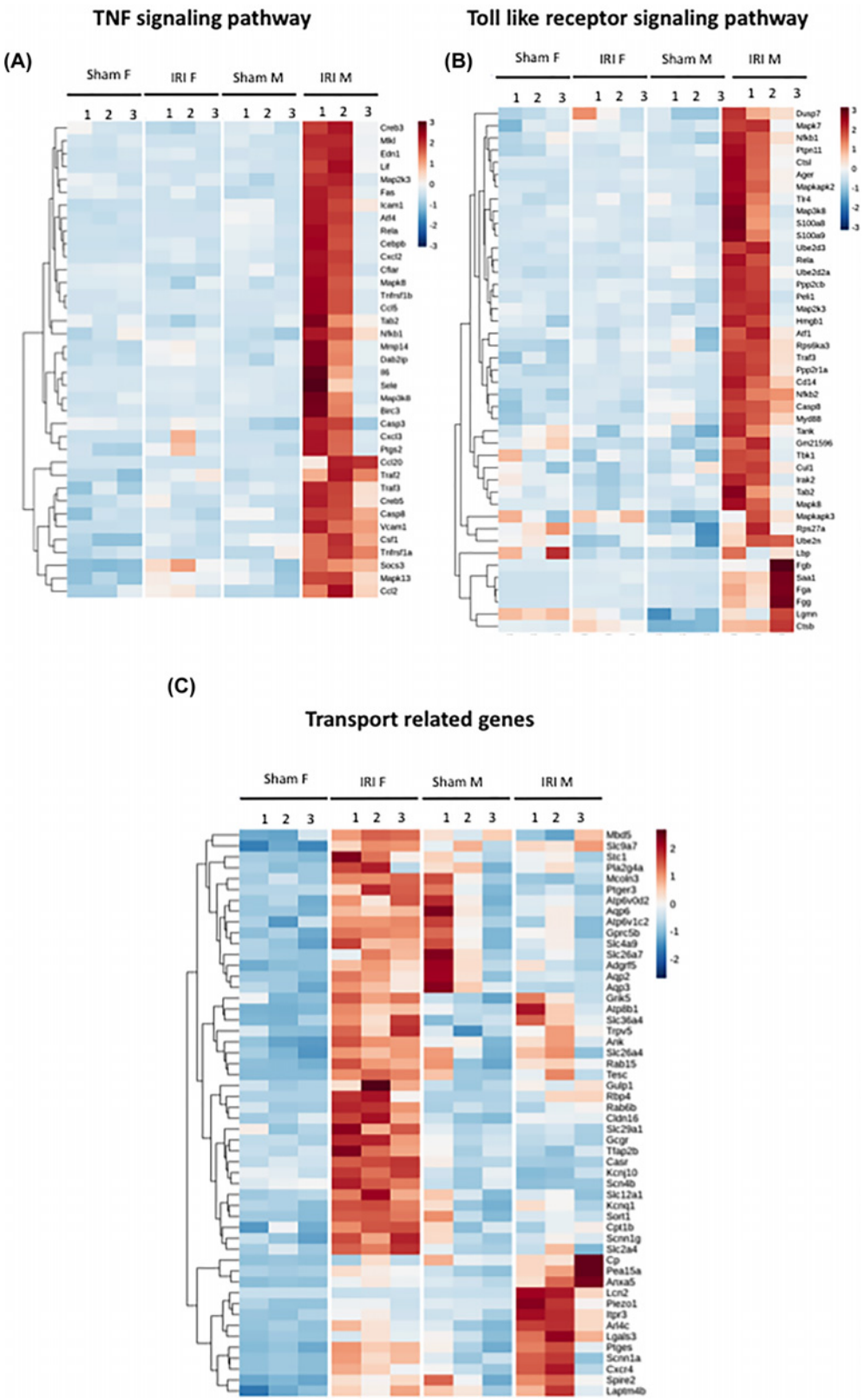

Figure 11. Heatmaps for differentially regulated genes (DEGs) from PTs after IRI in males and females

(**A**) Up-regulated genes linked to TNF signaling in males; (**B**) up-regulated genes involved in TLR signaling in males; (**C**) up-regulated genes linked to transport pathways in females. Hierarchical clustering of genes is shown at left of each heatmap, and z-score indicated by color; gene notation is shown at right of each map; n=3 per group.

Clinical Science (2020) **134** 1887–1909
https://doi.org/10.1042/CS20200168

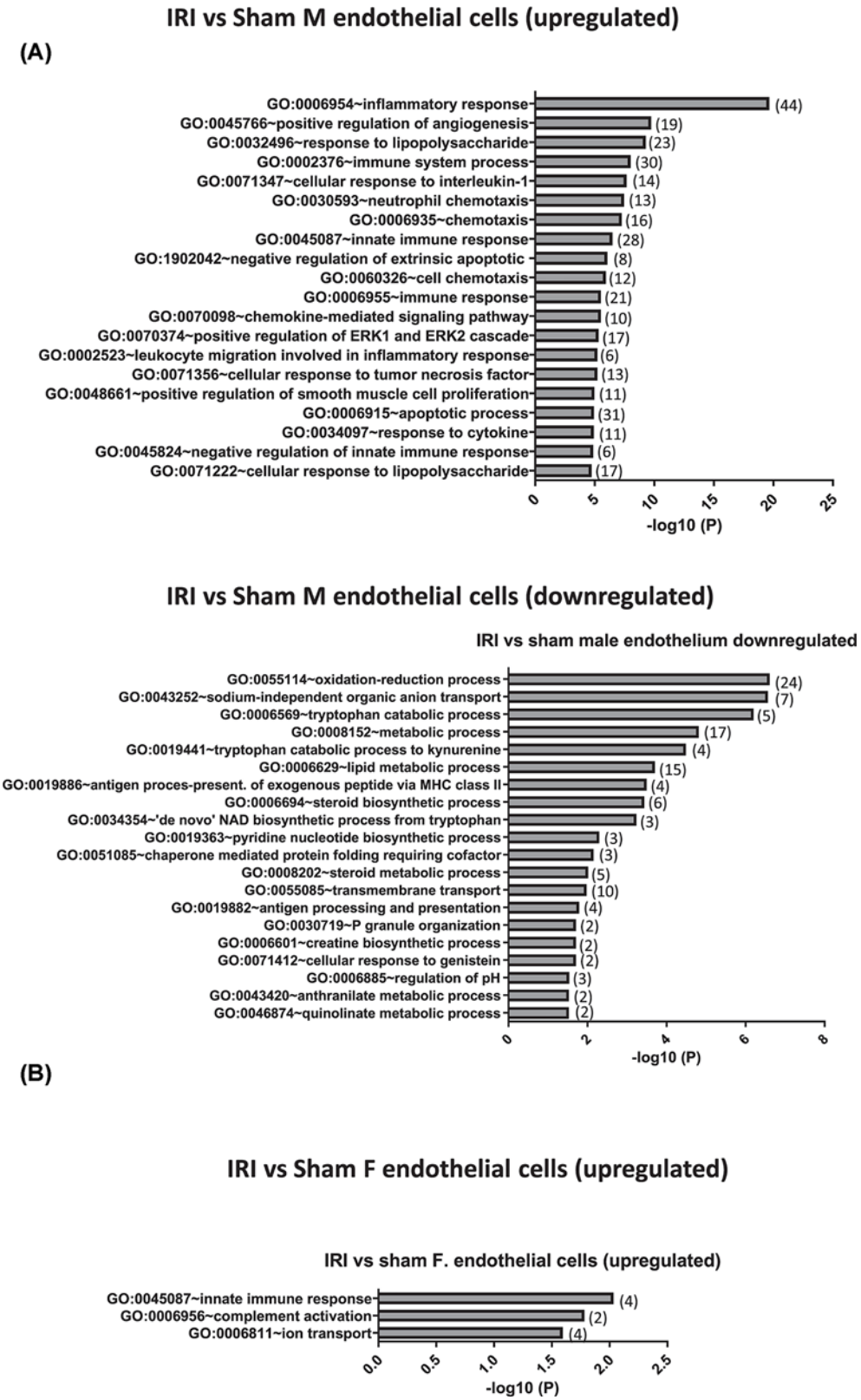

Figure 12. GO terms for up-regulated and down-regulated genes in endothelial cells after IRI

(**A**) Top 20 GO codes and terms for up-regulated and down-regulated genes from males are indicated, ranked according to level of significance, with number of genes in each term in parentheses. (**B**) Top three GO codes and terms for up-regulated genes from females are indicated, ranked according to level of significance, with number of genes in each term in parentheses.

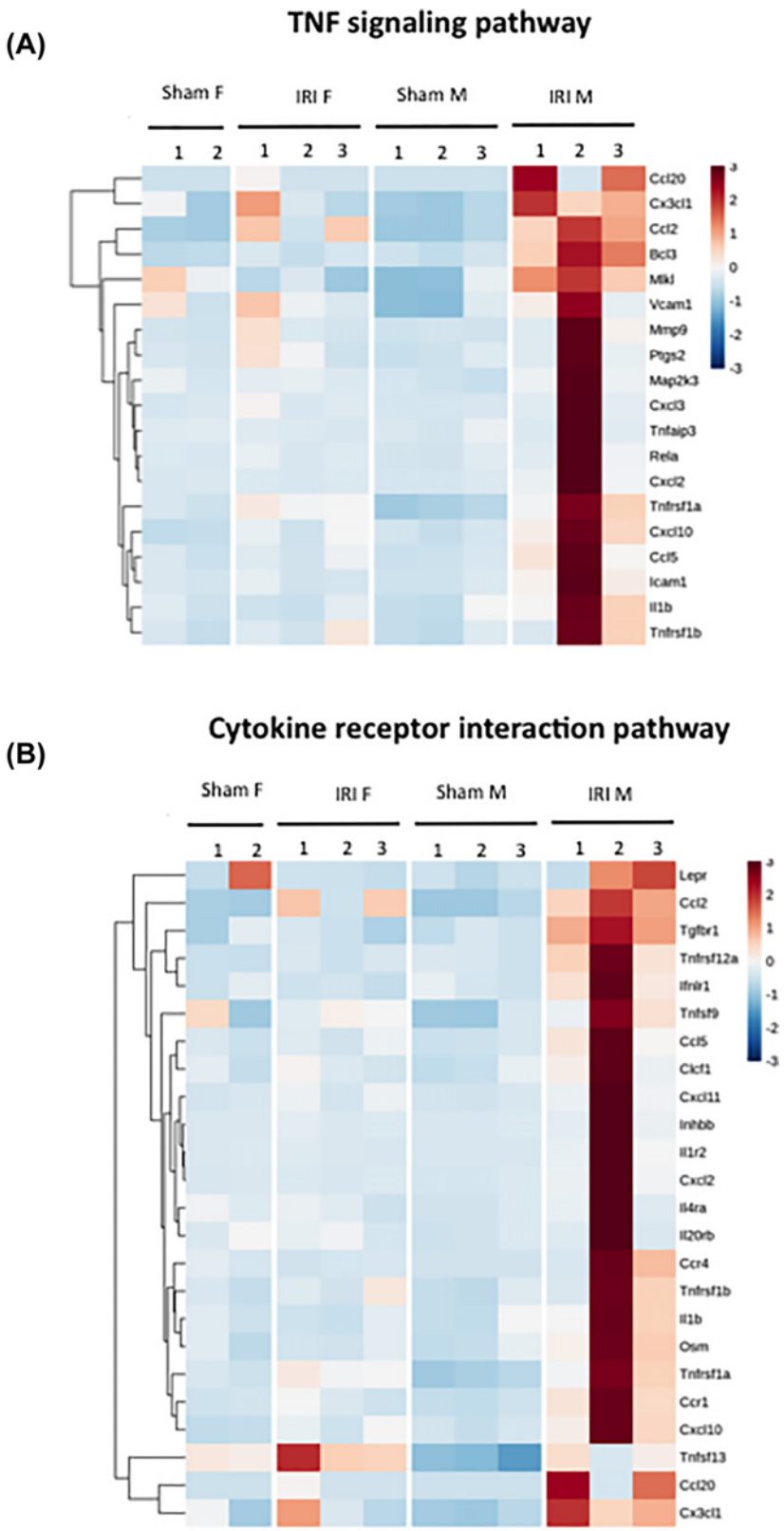

Figure 13. Heatmaps for differentially regulated genes (DEGs) from endothelial cells after IRI

(**A**) Up-regulated genes linked to TNF signaling in males; (**B**) up-regulated genes linked to cytokine receptor interaction in males. Hierarchical clustering of genes is shown at left of each heatmap, and z-score indicated by color; gene notation is shown at right of each map; *n*=3 per group, except for sham female endothelial cells (*n*=2).

Clinical Science (2020) **134** 1887–1909
https://doi.org/10.1042/CS20200168

with recent transcriptome profiling studies in mouse kidney [15,16], including predominance of cationic amino acid transporter *Slc7a12* and the *Prlr* in females, and increased expression of the cytochrome P450 gene *Cyp7b1* and fatty acid metabolism enzyme *Acsm3* in males. Interestingly, and also consistent with the results of Ransick et al. [15], enhanced expression of the estrogen receptor gene (*Esr1*) was observed in male PT. Sex disparities in PT gene expression in sham mice were linked to a variety of biological processes, and pathway analysis highlighted up-regulation of cytochrome P450/xenobiotic metabolism in females. Baseline sex differences in PT gene expression and biological processes could potentially contribute to disparities in susceptibility to ischemic AKI, although this requires further study.

With kidney IRI, PT gene expression in male mice was markedly dysregulated, with an almost ten-fold increase in DEGs compared with females. DEGs in male PTs included several rapidly activated genes linked to kidney IRI such as *Havcr, Lcn2,* and the keratin gene *Krt18,* a marker of renal epithelial cell injury [33]. In female PTs, these genes were less significantly activated. Furthermore, males alone demonstrated pronounced PT activation of *Krt20,* a gene with *de novo* expression in this segment in response to injury [29]. Male PTs showed enhanced relative expression of the EGF receptor gene compared with females after IRI, suggesting a potential role in predisposition to injury. In this regard, recent studies in mice and adult human kidneys demonstrated increased expression of the renal EGF receptor in males, which in mice is linked to progressive glomerulopathy and tubulointerstitial fibrosis [30]. Finally, *Sox9*, a transcription factor gene that is persistently activated for weeks after IRI and involved in tubular epithelial cell repair [34,35] was up-regulated in PTs from males, but not females.

Overall, the PT gene response in females with IRI was limited compared with males, except for up-regulation of certain transport-related genes. This up-regulation was unexpected, and may play a role in protection in females since tubular transport gene expression has been reported to decrease early after IRI, perhaps to limit energy consumption [36]. The limited gene response in females with IRI also correlated with decreased markers of injury, and suggests that molecular responses associated with chronic injury/repair are not activated. This interpretation is supported by significantly decreased megalin gene expression in males compared with females, as well as *Bcl2* expression. On the other hand, while the extent of apoptosis was increased in male kidneys, there was no difference in *Bax* gene expression between PTs from males and females after IRI, or in Bcl2 protein expression. These data suggest that changes in *Bax* or *Bcl2* may occur only transiently after reperfusion, or that post-translational modifications may account for altered protein expression as observed in our studies.

The pathogenesis of kidney IRI involves activation of inflammatory responses, and renal tubular cells contribute by elaborating proinflammatory cytokines, including interleukins and TNF-α [37]. Enhanced tubular cell TLR expression and signaling also exacerbates kidney IRI [38]. Pathway analysis and heatmaps revealed activation of PT genes involved in TNF and TLR signaling in males, but not females with IRI. Sex disparities in DEGs within these pathways were prominent and consistent with the limited neutrophil infiltration observed in female mice, and suggest that altered innate immune responses may underlie the difference in susceptibility to IRI.

Renal endothelial cells are critical targets of IRI, and become activated early, with production of proinflammatory cytokines, leukocyte adhesion, increased permeability, and altered vasomotor tone [39]. Endothelial regenerative capacity is also impaired in the renal vasculature after IRI, leading to vascular dropout [40]. A striking finding was that female mice exhibited only a small number of DEGs in endothelial cells after IRI (n=56) compared with males (n=1025). In agreement with previous studies [15], we observed marked up-regulation of *Inhbb*, the gene encoding the β-chain of inhibin B homodimers, a member of the transforming growth factor β (TGF-β) superfamily, in endothelial cells from males with IRI. The selective up-regulation of genes encoding adhesion molecules and cytokines/chemokines in male endothelial cells with IRI suggests that females are intrinsically protected from these early responses and are thereby less likely to experience ongoing hypoxic injury that contributes to vascular rarefaction and CKD. Consistent with this was the low number of DEGs in female endothelial cells, and the paucity of biological processes identified by GO.

A strength of our study is that two kidney cell types (PT and endothelium) critical to the pathogenesis of kidney IRI were specifically isolated for RNA-Seq, as opposed to transcriptome profiling on whole kidney homogenates. RNA-Seq also provided an unbiased approach to genes potentially mediating sex disparities in kidney IRI, which was validated with real time-PCR. Finally, we included data from three replicates per experimental group for RNA-Seq, which allowed for PCA and data segregation by group. We acknowledge certain limitations to the study. First, isolation of PTs and endothelial cells may have independently induced stress responses that could have affected gene signatures, although this limitation was mitigated by inclusion of control sham groups, and our PT data in sham mice is in good agreement with recent transcriptome analyses in healthy mouse kidneys [15,16]. Nonetheless, some variability in individual gene responses was observed in the three males with IRI. Second, we did not conduct RNA-Seq on all nephron segments, nor did we distinguish S1, S2 or S3 PTs. Other tubular segments as well as vascular cells, resident

fibroblasts or infiltrating inflammatory cells may contribute to sex disparities in IRI. Furthermore, since our RNA-Seq did not include translating ribosome affinity purification (TRAP), which can enhance the functionally importance of transcriptome profiles [16], our results must be considered as hypothesis-generating. Finally, the relevance of our findings to sex disparity in human ischemic AKI remains unclear. The data generated here is available from the Gene Expression Omnibus (GEO) repository (GSE144622) and can support additional studies on the functional impact of sex differences in individual genes.

Clinical perspectives

- AKI causes significant morbidity and mortality, and lacks effective treatments. In experimental animals and humans, males are more susceptible to AKI than females, although the molecular basis for this sex difference is unclear.
- Our RNA-Seq studies demonstrate sex-specific gene profiles in mouse PT and kidney endothelial cells with or without ischemia. Females exhibit markedly less activation of injury-associated genes with ischemia compared with males.
- These transcriptome data may help define biological processes that underlie sex differences in AKI susceptibility, and could lead to identification of therapeutic targets in humans with ischemic AKI.

Data Availability

The complete RNA-Seq dataset is available from the GEO repository (GSE144622). All data used for heatmaps and GO analysis are included in excel files (Supplementary Datasets S1 and S2).

Competing Interests

The authors declare that there are no competing interests associated with the manuscript.

Funding

This work was supported by the Canadian Institutes of Health Research [grant number 388364 (to K.D.B.)]; the Kidney Foundation of Canada [grant number 20170532 (to K.D.B.)]; and an unrestricted grant from the Russ and June Jones Family Foundation at The Ottawa Hospital (to K.D.B.).

Author Contribution

K.D.B. and J.L.V. conceived and designed the research plan. J.L.V., A.D., M.S., A.G., J.A.Z., K.T., and P.A.C. performed the experiments. J.L.V., M.S., A.G., C.J.P., and K.D.B. analyzed the data and interpreted the results. C.J.P. and J.L.V. performed bioinformatics analysis of the data. J.L.V., A.G., and C.J.P. prepared the figures. K.D.B. drafted the manuscript, with editing and revisions from J.L.V., A.D., and C.J.P. All authors approved the final version of the manuscript.

Acknowledgements

The technical support of StemCore Laboratories at the Ottawa Hospital Research Institute is gratefully acknowledged.

Abbreviations

Acsm3, acyl-CoA synthetase medium chain family member 3; AKI, acute kidney injury; Bax, Bcl-2-associated X protein; Bcl2, B-cell lymphoma 2; CD31, platelet endothelial cell adhesion molecule (cluster of differentiation 31); CKD, chronic kidney disease; Cldn1, claudin-1; Clu, clusterin; Cyp7b1, cytochrome P450 7B1; DEG, differentially expressed gene; GO, gene ontology; Havcr1, hepatitis A virus cellular receptor 1; Icam1, intercellular adhesion molecule 1; Inhbb, inhibin β B chain; IRI, ischemia–reperfusion injury; Krt18, keratin 18; Krt20, keratin 20; Kynu, kynureninase; Lcn2, lipocalin-2; Lrp2, low-density lipoprotein receptor-related protein 2; NGAL, neutrophil gelatinase-associated lipocalin; PCA, principal component analysis; PCR, polymerase chain reaction; Prlr, prolactin hormone receptor; PT, proximal tubule; RNA-Seq, RNA sequencing; Sele,

Clinical Science (2020) **134** 1887–1909
https://doi.org/10.1042/CS20200168

e-selectin; Slc22a30, solute carrier family 22, member 30; Slc7a12, solute carrier family 7, member 12; Sox9, SRY-Box transcription factor 9; TLR, toll-like receptor; TNF, tumor necrosis factor; TUNEL, terminal deoxynucleotidyl transferase-mediated dUTP nick-end labeling.

References

1 Negi, S., Koreeda, D., Kobayashi, S., Yano, T., Tatsuta, K., Mima, T. et al. (2018) Acute kidney injury: epidemiology, outcomes, complications, and therapeutic strategies. *Semin. Dial.* **31**, 519–527, https://doi.org/10.1111/sdi.12705
2 See, E.J., Jayasinghe, K., Glassford, N., Bailey, M., Johnson, D., Polkinghorne, K. et al. (2019) Long-term risk of adverse outcomes after acute kidney injury: a systematic review and meta-analysis of cohort studies using consensus definitions of exposure. *Kidney Int.* **95**, 160–172, https://doi.org/10.1016/j.kint.2018.08.036
3 Zuk, A. and Bonventre, J.V. (2016) Acute kidney injury. *Annu. Rev. Med.* **67**, 293–307, https://doi.org/10.1146/annurev-med-050214-013407
4 Kumar, S. (2018) Cellular and molecular pathways of renal repair after acute kidney injury. *Kidney Int.* **93**, 27–40, https://doi.org/10.1016/j.kint.2017.07.030
5 Basile, D.P. and Yoder, M.C. (2014) Renal endothelial dysfunction in acute kidney ischemia reperfusion injury. *Cardiovasc. Hematol. Disord. Drug Targets* **14**, 3–14, https://doi.org/10.2174/1871529X1401140724093505
6 de Caestecker, M., Humphreys, B.D., Liu, K.D., Fissell, W.H., Cerda, J., Nolin, T.D. et al. (2015) Bridging translation by improving preclinical study design in AKI. *J. Am. Soc. Nephrol.* **26**, 2905–2916, https://doi.org/10.1681/ASN.2015070832
7 Park, K.M., Kim, J.I., Ahn, Y., Bonventre, A.J. and Bonventre, J.V. (2004) Testosterone is responsible for enhanced susceptibility of males to ischemic renal injury. *J. Biol. Chem.* **279**, 52282–52292, https://doi.org/10.1074/jbc.M407629200
8 Kher, A., Meldrum, K.K., Wang, M., Tsai, B.M., Pitcher, J.M. and Meldrum, D.R. (2005) Cellular and molecular mechanisms of sex differences in renal ischemia–reperfusion injury. *Cardiovasc. Res.* **67**, 594–603, https://doi.org/10.1016/j.cardiores.2005.05.005
9 Satake, A., Takaoka, M., Nishikawa, M., Yuba, M., Shibata, Y., Okumura, K. et al. (2008) Protective effect of 17beta-estradiol on ischemic acute renal failure through the PI3K/Akt/eNOS pathway. *Kidney Int.* **73**, 308–317, https://doi.org/10.1038/sj.ki.5002690
10 Kang, K.P., Lee, J.E., Lee, A.S., Jung, Y.J., Kim, D., Lee, S. et al. (2014) Effect of gender differences on the regulation of renal ischemia-reperfusion-induced inflammation in mice. *Mol. Med. Rep.* **9**, 2061–2068, https://doi.org/10.3892/mmr.2014.2089
11 Neugarten, J., Golestaneh, L. and Kolhe, N.V. (2018) Sex differences in acute kidney injury requiring dialysis. *BMC Nephrol.* **19**, 131, https://doi.org/10.1186/s12882-018-0937-y
12 Neugarten, J. and Golestaneh, L. (2018) Female sex reduces the risk of hospital-associated acute kidney injury: a meta-analysis. *BMC Nephrol.* **19**, 314, https://doi.org/10.1186/s12882-018-1122-z
13 Fekete, A., Vannay, A., Vér, A., Rusai, K., Müller, V., Reusz, G. et al. (2006) Sex differences in heat shock protein 72 expression and localization in rats following renal ischemia-reperfusion injury. *Am. J. Physiol. Renal Physiol.* **291**, F806–F811, https://doi.org/10.1152/ajprenal.00080.2006
14 Tanaka, R., Tsutsui, H., Kobuchi, S., Sugiura, T., Yamagata, M., Ohkita, M. et al. (2012) Protective effect of 17β-estradiol on ischemic acute kidney injury through the renal sympathetic nervous system. *Eur. J. Pharmacol.* **683**, 270–275, https://doi.org/10.1016/j.ejphar.2012.02.044
15 Ransick, A., Lindström, N.O., Liu, J., Zhu, Q., Guo, J.J., Alvarado, G.F. et al. (2019) Single-cell profiling reveals sex, lineage, and regional diversity in the mouse kidney. *Dev. Cell* **51**, 399–413, https://doi.org/10.1016/j.devcel.2019.10.005
16 Wu, H., Lai, C.F., Chang-Panesso, M. and Humphreys, B.D. (2020) Proximal tubule translational profiling during kidney fibrosis reveals proinflammatory and long noncoding RNA expression patterns with sexual dimorphism. *J. Am. Soc. Nephrol.* **31**, 23–38, https://doi.org/10.1681/ASN.2019040337
17 Burger, D., Viñas, J.L., Akbari, S., Dehak, H., Knoll, W., Gutsol, A. et al. (2015) Human endothelial colony-forming cells protect against acute kidney injury: role of exosomes. *Am. J. Pathol.* **185**, 2309–2323, https://doi.org/10.1016/j.ajpath.2015.04.010
18 Viñas, J.L., Burger, D., Zimpelmann, J., Haneef, R., Knoll, W., Campbell, P. et al. (2016) Transfer of microRNA-486-5p from human endothelial colony forming cell-derived exosomes reduces ischemic kidney injury. *Kidney Int.* **90**, 1238–1250, https://doi.org/10.1016/j.kint.2016.07.015
19 Viñas, J.L., Spence, M., Gutsol, A., Knoll, W., Burger, D., Zimpelmann, J. et al. (2018) Receptor-ligand interaction mediates targeting of endothelial colony forming cell-derived exosomes to the kidney after ischemic injury. *Sci. Rep.* **8**, 16320, https://doi.org/10.1038/s41598-018-34557-7
20 Pfaffl, M.W. (2001) A new mathematical model for relative quantification in real-time RT-PCR. *Nucleic Acids Res.* **29**, e45, https://doi.org/10.1093/nar/29.9.e45
21 Patro, R., Duggal, G., Love, M.I., Irizarry, R.A. and Kingsford, C. (2017) Salmon provides fast and bias-aware quantification of transcript expression. *Nat. Methods* **14**, 417–419, https://doi.org/10.1038/nmeth.4197
22 Soneson, C., Love, M. and Robinson, M.D. (2015) Differential analyses for RNA-seq: transcript-level estimates improve gene-level inferences. Version 2. *F1000Res.* **4**, 1521, https://doi.org/10.12688/f1000research.7563.1
23 Love, M.I., Huber, W. and Anders, S. (2014) Moderated estimation of fold change and dispersion for RNA-seq data with DESeq2. *Genome Biol.* **15**, 550, https://doi.org/10.1186/s13059-014-0550-8
24 Zhu, A., Ibrahim, J.G. and Love, M.I. (2019) Heavy-tailed prior distributions for sequence count data: removing the noise and preserving large differences. *Bioinformatics* **35**, 2084–2092, https://doi.org/10.1093/bioinformatics/bty895
25 Dennis, Jr, G., Sherman, B.T., Hosack, D.A., Yang, J., Gao, W., Lane, H.C. et al. (2003) DAVID: Database for Annotation, Visualization, and Integrated Discovery. *Genome Biol.* **4**, P3, https://doi.org/10.1186/gb-2003-4-5-p3
26 Schreiber, A., Theilig, F., Schweda, F. and Höcherl, K. (2012) Acute endotoxemia in mice induces downregulation of megalin and cubilin in the kidney. *Kidney Int.* **82**, 53–59, https://doi.org/10.1038/ki.2012.62
27 Kumar, S., Liu, J. and McMahon, A.P. (2014) Defining the acute kidney injury and repair transcriptome. *Semin. Nephrol.* **34**, 404–417, https://doi.org/10.1016/j.semnephrol.2014.06.007

28 Liu, J., Krautzberger, A.M., Sui, S.H., Hofmann, O.M., Chen, Y., Baetscher, M. et al. (2014) Cell-specific translational profiling in acute kidney injury. *J. Clin. Invest.* **124**, 1242–1254, https://doi.org/10.1172/JCI72126
29 Liu, J., Kumar, S., Dolzhenko, E., Alvarado, G.F., Guo, J., Lu, C. et al. (2017) Molecular characterization of the transition from acute to chronic kidney injury following ischemia/reperfusion. *JCI Insight* **21**, e94716, https://doi.org/10.1172/jci.insight.94716
30 Zhang, M.Z., Sasaki, K., Li, Y., Li, Z., Pan, Y., Jin, G.N. et al. (2019) The role of the EGF receptor in sex differences in kidney injury. *J. Am. Soc. Nephrol.* **30**, 1659–1673, https://doi.org/10.1681/ASN.2018121244
31 Tran, M., Tam, D., Bardia, A., Bhasin, M., Rowe, G.C., Kheret, A. et al. (2011) PGC-1α promotes recovery after acute kidney injury during systemic inflammation in mice. *J. Clin. Invest.* **121**, 4003–4014, https://doi.org/10.1172/JCI58662
32 Poyan Mehr, A., Tran, M.T., Ralto, K.M., Leaf, D.E., Washco, V., Messmer, J. et al. (2018) De novo NAD+ biosynthetic impairment in acute kidney injury in humans. *Nat. Med.* **24**, 1351–1359, https://doi.org/10.1038/s41591-018-0138-z
33 Djudjaj, S., Papasotiriou, M., Bülow, R.D., Wagnerova, A., Lindenmeyer, M.T., Cohen, C.D. et al. (2016) Keratins are novel markers of renal epithelial cell injury. *Kidney Int.* **89**, 792–808, https://doi.org/10.1016/j.kint.2015.10.015
34 Kumar, S., Liu, J., Pang, P., Krautzberger, A.M., Reginensi, A., Akiyama, H. et al. (2015) Sox9 activation highlights a cellular pathway of renal repair in the acutely injured mammalian kidney. *Cell Rep.* **12**, 1325–1338, https://doi.org/10.1016/j.celrep.2015.07.034
35 Kang, H.M., Huang, S., Reidy, K., Han, S.H., Chinga, F. and Susztak, K. (2016) Sox9-positive progenitor cells play a key role in renal tubule epithelial regeneration in mice. *Cell Rep.* **14**, 861–871, https://doi.org/10.1016/j.celrep.2015.12.071
36 Fattah, H. and Vallon, V. (2018) Tubular recovery after acute kidney injury. *Nephron* **140**, 140–143, https://doi.org/10.1159/000490007
37 Sharfuddin, A.A. and Molitoris, B.A. (2011) Pathophysiology of ischemic acute kidney injury. *Nat. Rev. Nephrol.* **7**, 189–200, https://doi.org/10.1038/nrneph.2011.16
38 Wu, H., Chen, G., Wyburn, K.R., Yin, J., Bertolino, P., Eris, J.M. et al. (2007) TLR4 activation mediates kidney ischemia/reperfusion injury. *J. Clin. Invest.* **117**, 2847–2859, https://doi.org/10.1172/JCI31008
39 Verma, S.K. and Molitoris, B.A. (2015) Renal endothelial injury and microvascular dysfunction in acute kidney injury. *Semin. Nephrol.* **35**, 96–107, https://doi.org/10.1016/j.semnephrol.2015.01.010
40 Basile, D.P., Friedrich, J.L., Spahic, J., Knipe, N., Mang, H., Leonard, E.C. et al. (2011) Impaired endothelial proliferation and mesenchymal transition contribute to vascular rarefaction following acute kidney injury. *Am. J. Physiol. Renal Physiol.* **300**, F721–F733, https://doi.org/10.1152/ajprenal.00546.2010

S1

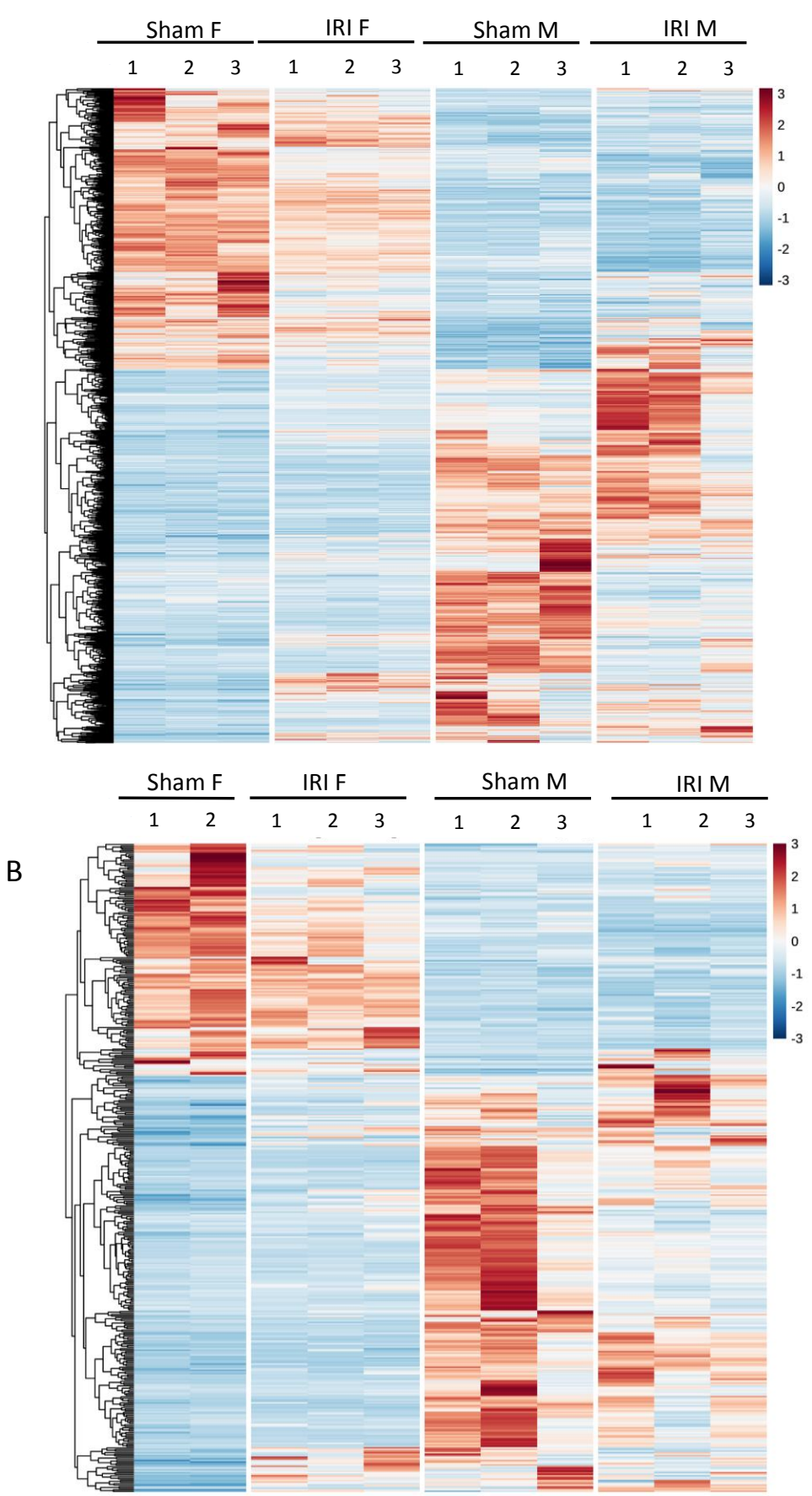

S1. Heat maps for differentially regulated genes (DEGs) from sham male (Sham M) mice compared to sham female (Sham F) mice. A) Heat map for proximal tubular DEGs (1,800 genes). B) Heat map for endothelial cell DEGs (418 genes). Hierarchical clustering of genes indicated at left of each heatmap, and z-score indicated by color; n=3 per group except for sham female endothelial cells (n=2).

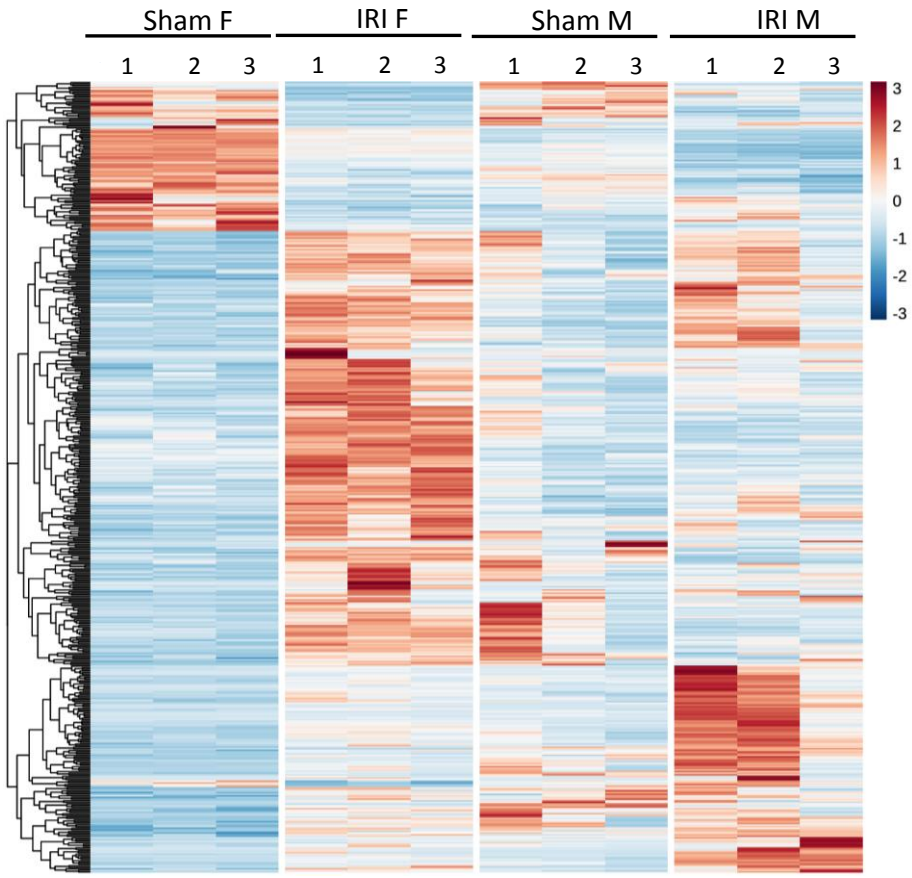

S2. Heat map for 488 differentially regulated genes (DEGs) in IRI female mice (IRI F) compared to sham female mice (Sham F) for proximal tubular cells. Hierarchical clustering of genes indicated at left of each heatmap, and z-score indicated by color; n=3 per group.

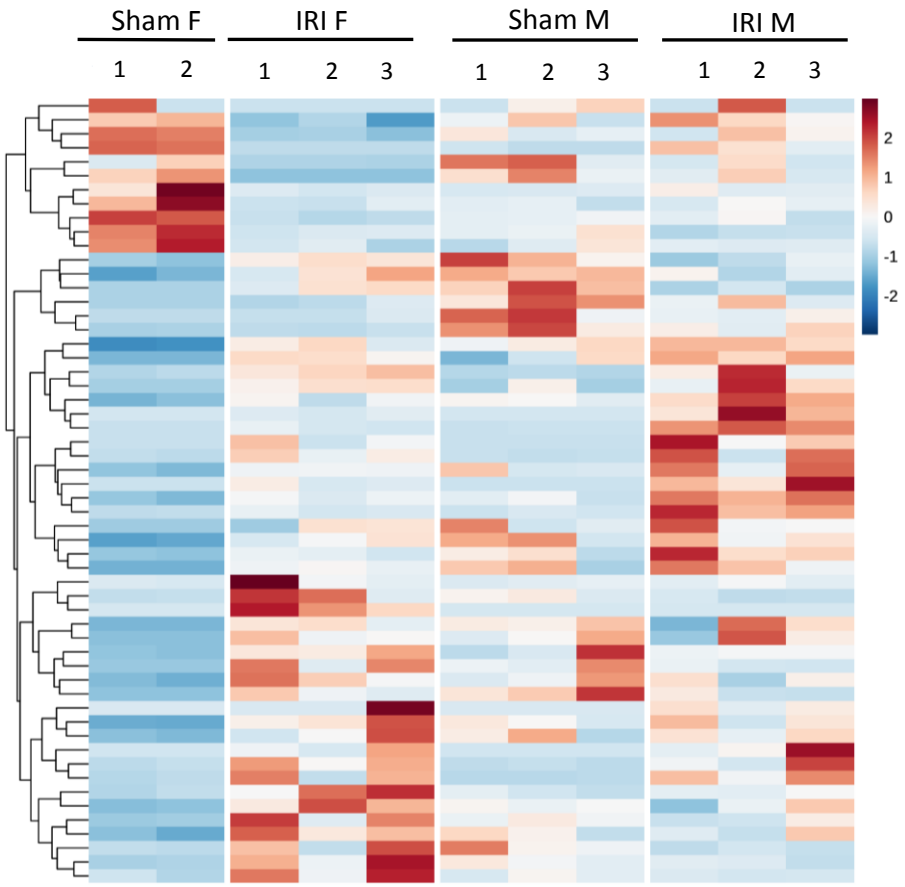

S3. Heat map for 56 differentially regulated genes (DEGs) in endothelial cells from IRI female mice (IRI F) compared to sham female mice (Sham F). Hierarchical clustering of genes indicated at left of each heatmap, and z-score indicated by color; n=3 per group except for sham female endothelial cells (n=2).

S4

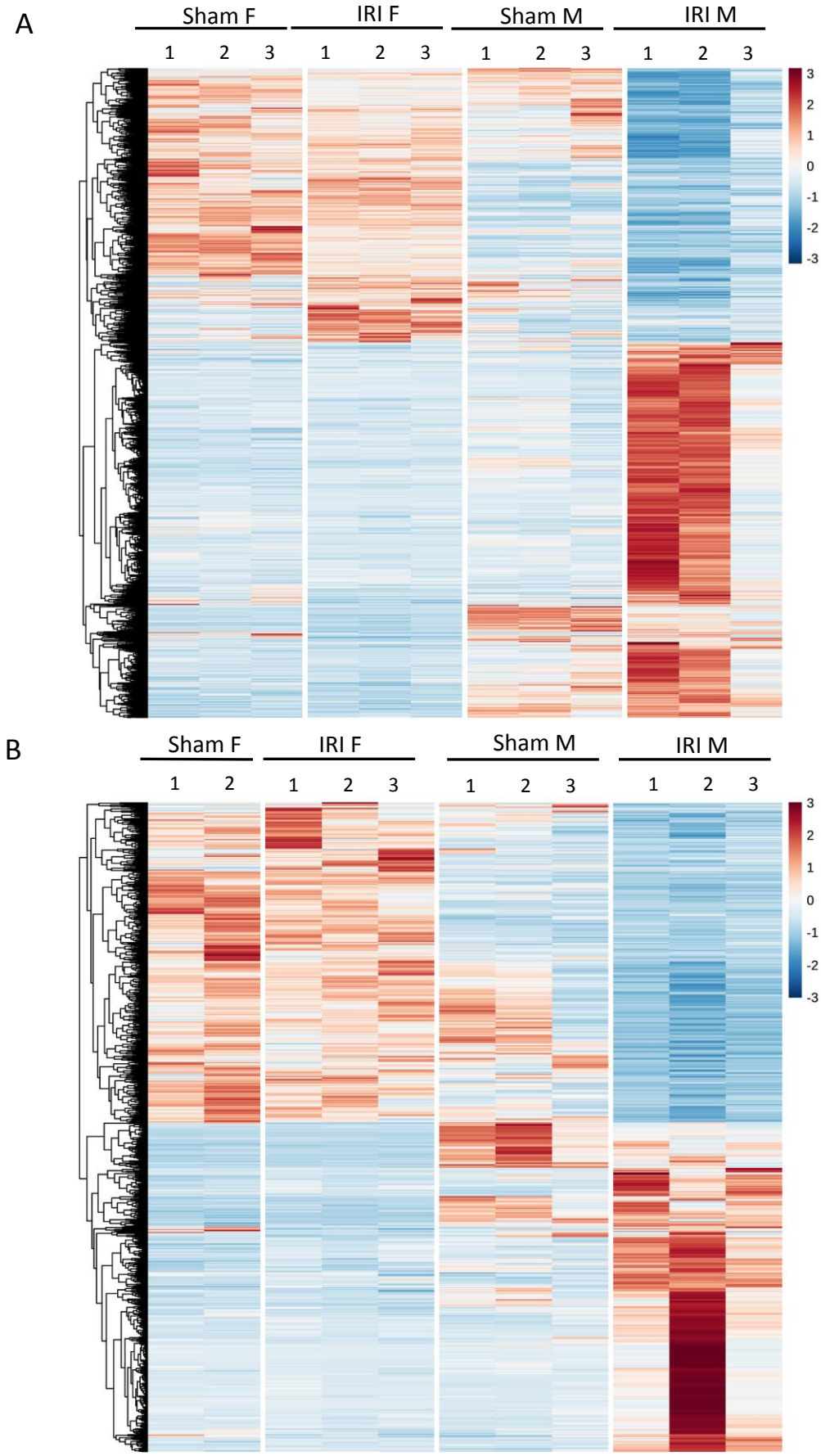

<u>S4</u>. Heat maps for differentially regulated genes (DEGs) in IRI male mice (IRI M) compared to IRI female mice (IRI F). A) Heat map for proximal tubular cell DEGs (4,557 genes). B) Heat map for endothelial cell DEGs (992 genes). Hierarchical clustering of genes indicated at left of each heatmap, and z-score indicated by color; n=3 per group except for sham female endothelial cells (n=2).

A

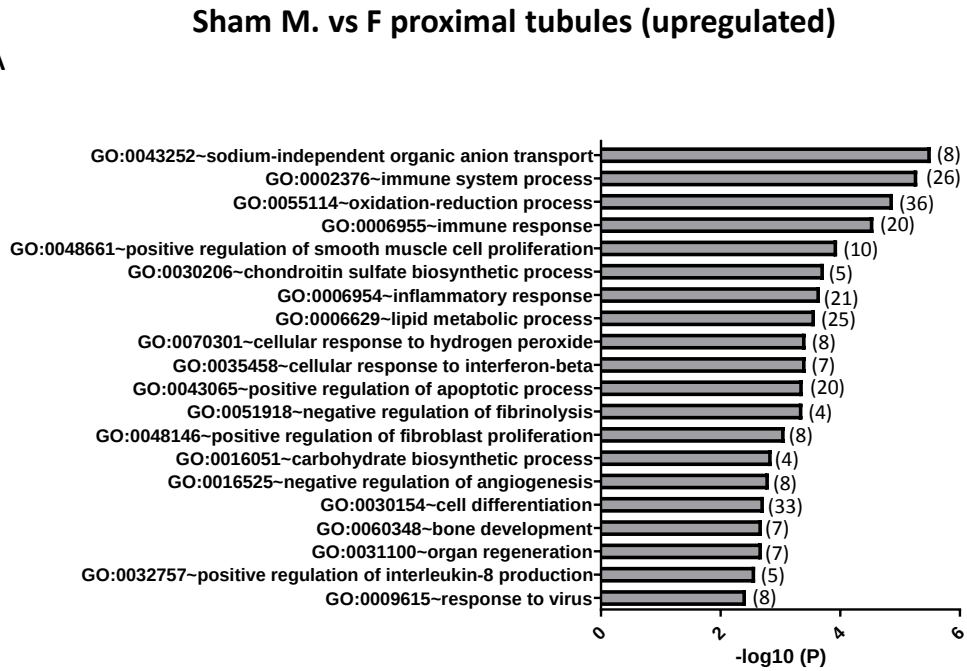

B

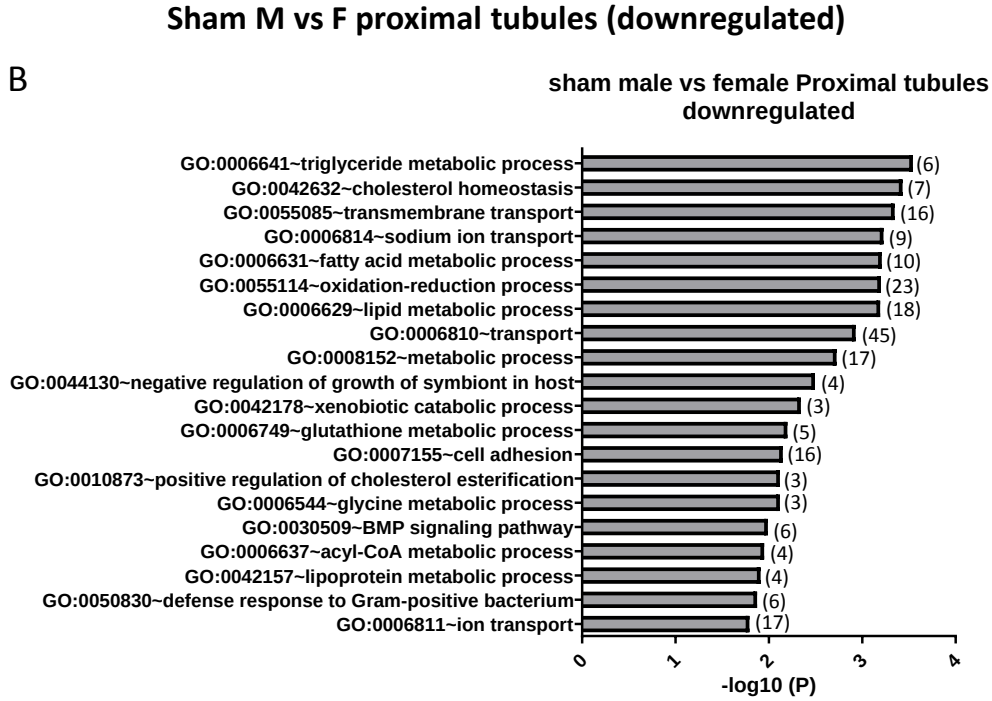

S5. Gene ontology (GO) analysis for upregulated and downregulated differentially regulated genes (DEGs) in proximal tubular cells from sham male mice compared to sham female mice. A) Top 20 GO codes for upregulated genes from males ranked according to level of significance, with number of genes in each term in parentheses. B) Top 20 GO codes for downregulated genes from males ranked according to level of significance, with number of genes in each term in parentheses.

S6

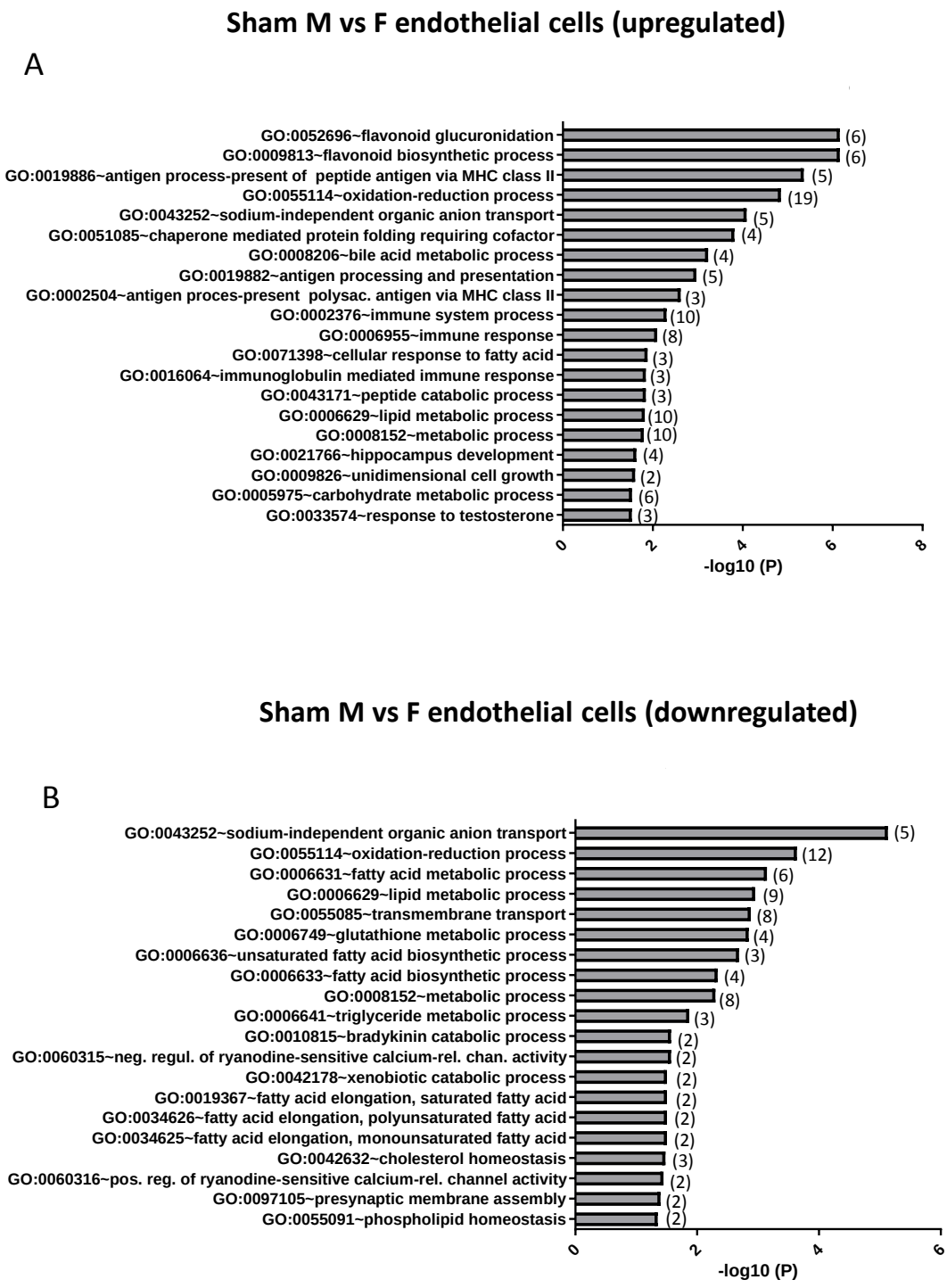

S6. Gene ontology (GO) analysis for upregulated and downregulated differentially regulated genes (DEGs) in endothelial cells from sham male mice compared to sham female mice. A) Top 20 GO codes for upregulated genes from males ranked according to level of significance, with number of genes in each term in parentheses. B) Top 20 GO codes for downregulated genes from males ranked according to level of significance, with number of genes in each term in parentheses.

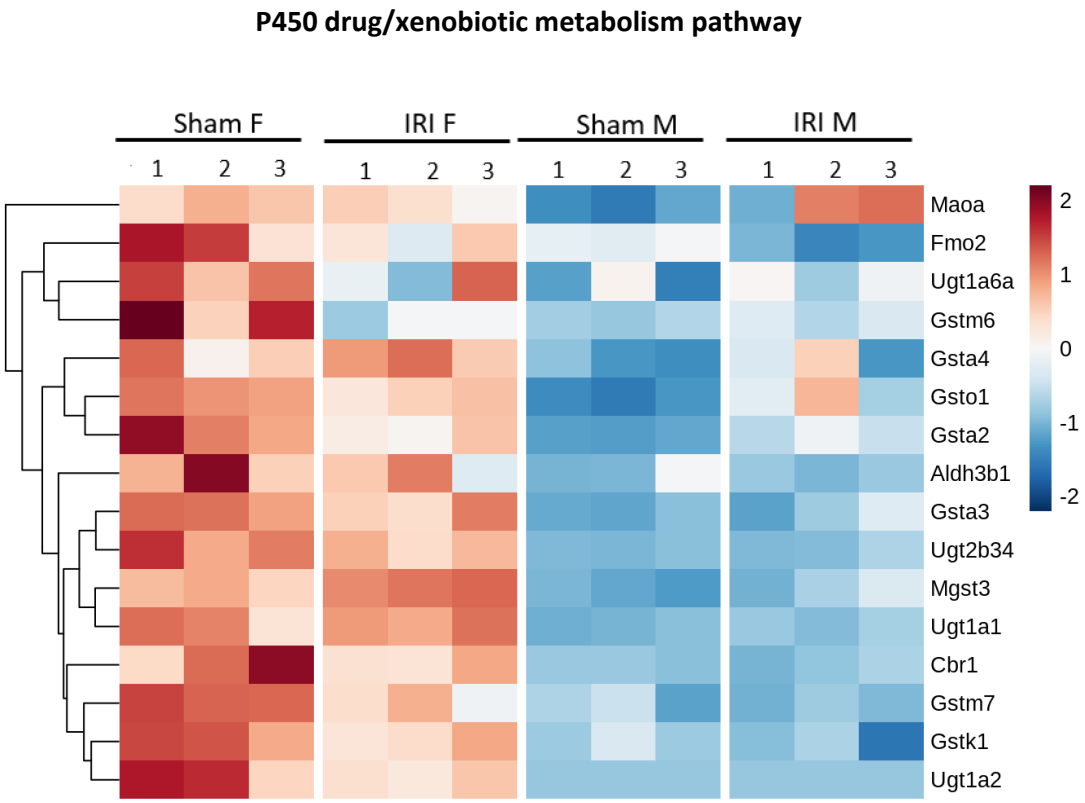

S7. Heat map showing upregulated genes related to the P450 drug/xenobiotic metabolism pathway in sham female proximal tubular cells (Sham F) compared to sham male (Sham M); Differentially regulated genes (DEGs) (16 genes). Hierarchical clustering of genes indicated at left of each heatmap, and z-score indicated by color; n=3 per group.